antioxidants

MDPI

Article

Formulation and Biological Evaluation of *Glycyrrhiza glabra* L. Methanolic Extract: An Exploratory Study in the Context of Rosacea

Iulia Semenescu [1,2], Larisa Bora [1,2], Adina Octavia Duse [3,4,*], Claudia Geanina Watz [5,6,7], Ștefana Avram [1,2,*], Szilvia Berkó [8], Gheorghe Emilian Olteanu [6,9], Adina Căta [10], Zorița Diaconeasa [11], Daliana Ionela Minda [1,2], Cristina Adriana Dehelean [6,12], Delia Muntean [13,14] and Corina Danciu [1,2]

1 Department of Pharmacognosy-Phytotherapy, "Victor Babeș" University of Medicine and Pharmacy, Eftimie Murgu Square, No. 2, 300041 Timișoara, Romania; iulia.semenescu@umft.ro (I.S.); larisa.bora@umft.ro (L.B.); daliana.minda@umft.ro (D.I.M.); corina.danciu@umft.ro (C.D.)
2 Research and Processing Center of Medicinal and Aromatic Plants, "Victor Babeș" University of Medicine and Pharmacy Timișoara, Eftimie Murgu Square, No. 2, 300041 Timișoara, Romania
3 Department of Rehabilitation, Physical Medicine and Rheumatology, Faculty of Medicine, "Victor Babeș" University of Medicine and Pharmacy Timișoara, Eftimie Murgu Square, No. 2, 300041 Timișoara, Romania
4 Municipal Clinical Emergency Hospital, 300254 Timișoara, Romania
5 Department of Pharmaceutical Physics, Faculty of Pharmacy, "Victor Babeș" University of Medicine and Pharmacy Timișoara, Eftimie Murgu Square, No. 2, 300041 Timișoara, Romania; farcas.claudia@umft.ro
6 Research Center for Pharmaco-Toxicological Evaluation, "Victor Babeș" University of Medicine and Pharmacy Timișoara, Eftimie Murgu Square, No. 2, 300041 Timișoara, Romania; olteanu.gheorghe@umft.ro (G.E.O.); cadehelean@umft.ro (C.A.D.)
7 OncoGen Center for Gene and Cellular Therapies in the Treatment of Cancer, "Pius Brînzeu" County Clinical, Emergency Hospital Timișoara, Blvd. Liviu Rebreanu, 156, 300723 Timișoara, Romania
8 Institute of Pharmaceutical Technology and Regulatory Affairs, Faculty of Pharmacy, University of Szeged, Eötvös u. 6, H-6720 Szeged, Hungary; berko.szilvia@szte.hu
9 Department of Infectious Diseases, Discipline of Pulmonology, Center for Research and Innovation in Personalized Medicine of Respiratory Diseases, Eftimie Murgu Square, No. 2, 300041 Timișoara, Romania
10 National Institute of Research and Development for Electrochemistry and Condensed Matter, 144 Dr. A. P. Podeanu, 300569 Timișoara, Romania; adina.cata@incemc.ro
11 Department of Food Science and Technology, Faculty of Food Science and Technology, University of Agricultural Science and Veterinary Medicine, Calea Manastur, 3-5, 400372 Cluj-Napoca, Romania; zorita.sconta@usamvcluj.ro
12 Department of Toxicology and Drug Industry, "Victor Babeș" University of Medicine and Pharmacy Timișoara, Eftimie Murgu Square, No. 2, 300041 Timișoara, Romania
13 Department of Microbiology, Faculty of Medicine, "Victor Babeș" University of Medicine and Pharmacy Timișoara, Eftimie Murgu Square, No. 2, 300041 Timișoara, Romania; muntean.delia@umft.ro
14 Multidisciplinary Research Center on Antimicrobial Resistance, "Victor Babeș" University of Medicine and Pharmacy Timișoara, Eftimie Murgu Square, No. 2, 300041 Timișoara, Romania
* Correspondence: duse.adina@umft.ro (A.O.D.); stefana.avram@umft.ro (Ș.A.)

Abstract

Rosacea is a chronic inflammatory skin disorder characterized by oxidative stress, innate immune dysregulation, vascular instability, and microbiome-related triggers. *Glycyrrhiza glabra* (Gg, licorice) root contains phenolics and triterpenoids with antioxidant, anti-inflammatory, antimicrobial, and anti-angiogenic properties that may benefit rosacea-prone skin. Xanthan-gum hydrogels containing 2% methanolic Gg extract (S1, S2) were prepared and characterized. Rheology, in vitro release, and in vitro permeation were evaluated, with the aim of assessing their suitability as topical formulations for rosacea-prone skin. Antioxidant activity was assessed using DPPH, ABTS, and FRAP assays. Antimicrobial effects were tested against *S. pyogenes*, *S. aureus*, and *C. acnes*. Safety and bioactivity were examined through HaCaT keratinocyte assays (MTT, Neutral Red, LDH), the HET-CAM irritation test, and the CAM angiogenesis assay. Immunocytochemistry was performed on rosacea-related inflammatory markers. Both hydrogels showed suitable rheology, sustained

Check for updates

Academic Editor: Alessandra Napolitano

Received: 19 December 2025
Revised: 14 January 2026
Accepted: 20 January 2026
Published: 23 January 2026

Copyright: © 2026 by the authors. Licensee MDPI, Basel, Switzerland. This article is an open access article distributed under the terms and conditions of the Creative Commons Attribution (CC BY) license.

release, and preserved strong antioxidant activity. Moderate antimicrobial effects were observed, particularly against *S. pyogenes* and *C. acnes*. HaCaT cell viability remained above 84% for the S2 formulation at the highest concentration (200 µg/mL), indicating improved cytocompatibility compared with formulation S1. The hydrogels were non-irritant in the HET-CAM model and reduced neovascularization in the CAM assay, with a more sustained effect observed for formulation S2. Immunohistochemistry supported potential modulation of inflammatory pathways relevant to rosacea, evidencing suppressed VEGF expression and preserved CD44-mediated integrity, particularly in the Labrasol-based formulation (S2), while Caspase-3 staining indicated a controlled apoptotic profile. Overall, Gg hydrogels are safe, biocompatible, non-irritant, and exhibit antioxidant, antimicrobial, and anti-angiogenic activities, supporting their potential as biocompatible topical formulations with antioxidant and pathway-modulating properties relevant to the biological features associated with rosacea, while underscoring the importance of formulation design.

Keywords: *Glycyrrhiza glabra*; root; methanolic extracts; hydrogels; antioxidant; antimicrobial; HaCaT keratinocytes; angiogenesis; imunohistochemistry

1. Introduction

Rosacea is a chronic skin disorder that is mainly characterized by three hallmarks: erythema, telangiectasias, and inflammation. Sometimes, pustules and papules are also present. It is usually accompanied by sensations of stinging, burning, and/or flushing, that can exacerbate in different situations. Even though the incidence of this skin condition is continuously increasing, and the social and psychological impact are significant, there is still insufficient information about its pathogenesis [1]. Some factors that are known to contribute to the appearance of rosacea include a dysfunctional epidermal barrier, genetic susceptibility, pilosebaceous unit abnormalities, vascular alterations, and microbial organisms [2].

The treatment of rosacea mainly consists of topical agents like azelaic acid, metronidazole, benzoyl peroxide, or brimonidine gel, and can be further implemented with oral antibiotics like doxycycline or minocycline [3,4]. Recent studies show that a combination of the two usually yields better results [3]. However, their precise role within the rosacea disease process remains unclear, given the incomplete understanding of rosacea pathophysiology. It is believed that their clinical efficacy may be attributed mainly to their anti-inflammatory or anti-angiogenic properties [5].

Elevated expression of Toll-like receptor 2 (TLR2), cathelicidin antimicrobial peptide (Camp), and kallikrein 5 (KLK5) were observed in rosacea skin lesions [6]. Moreover, in a recent study, Li Y et al. [7] showed that inhibition of KLK5 improved erythema and inflammation in this skin condition. The innate immune cells' infiltration, including macrophages, neutrophils, and mast cells, was also observed in rosacea [8].

After several decades of supremacy of synthetic medication, culminating with the emergence of antibiotic resistance, herbal medicine tends to regain popularity [9]. The World Health Organization (WHO) appreciates the importance of plant remedies and encourages the use of phytotherapy in order to obtain new drugs with superior efficacy, quality, and safety [10]. In the context of rosacea—where oxidative stress, inflammation, and vascular dysfunction coexist—plant-derived formulations with antioxidant, anti-inflammatory, and vasoregulatory properties represent a rational area of investigation [11]. Moreover, the synergistic action of multiple phytochemicals within plant extracts has been shown to enhance both efficacy and safety profiles [12].

Glycyrrhiza glabra L. (Gg) is a medicinal plant that has attracted the attention of researchers due to its complex composition and multiple therapeutic effects. Phytochemical screening of the licorice root shows a complex of around 400 compounds [13]. These compounds belong to various phytochemical classes: triterpenes, saponins, flavonoids, phenolic compounds, alkaloids, and others [13,14]. The most important secondary metabolites are triterpene saponins (glycyrrhizin), flavanone glycosides (liquiritin), isoflavonoids (glabradin), chalcone glycosides (isoliquiritin), and various types of free phenolic compounds [15]. Glycyrrhizin is the main saponin ingredient, constituting between 10 and 25% of the licorice root extract [16]. Glycyrrhizic acid, the glycyrrhizin aglycone, is normally considered the main bioactive compound [17]. Both glycyrrhizin and glycyrrhizic acid have been intensively studied for their anti-inflammatory activity and ability to reduce ROS [17]. The main representatives of the isoflavone class, glabridin and hispaglabridins A and B, are compounds with estrogen-like and antioxidant activity [18].

It is well known that the composition of licorice extract differs depending on the type of solvents used. Previous studies have shown that the extract obtained with pure methanol contains the largest number of bioactive compounds, including acids (3,4-dihydroxybenzoic, caffeic, chlorogenic, n-coumaric, ferulic, chicory, and rosmarinic acid), rutin, luteolin, astragalin, hesperetin, apigenin, and others [19]. The methanolic licorice extract also yields greater amount of glycyrrhizin compared to the ethanolic extract, with better antioxidant and antimicrobial activities [20].

The methanolic Gg root extract investigated in this study was previously phytochemically characterized by our group, allowing both the identification and quantification of major constituents, with glycyrrhizin as the predominant compound (13.927 mg/g dry extract), alongside flavonoids such as liquiritin, liquiritigenin derivatives, and apigenin- and luteolin-based glycosides, thus providing a chemically standardized basis for the present biological evaluation [21].

There are several clinical studies that evaluate the role of different phytochemicals in the management of rosacea [22]. While the majority of these studies focus on general plant-derived compounds, for their important antioxidant and anti-inflammatory proprieties [1,23], limited data specifically address the potential of Gg in the control of this skin disorder. Still, in vitro findings show that Gg extracts can inhibit pro-inflammatory cytokines such as IL-6 and TNF-α, and reduce ROS production by inhibiting key signaling pathways such as NF-κB and MAPKs [24], suppressing proinflammatory cytokines, highlighting their biological relevance in the management of inflammatory disorders.

Considering the multiple therapeutic properties mentioned previously, many of which relate to biological mechanisms currently recognized for rosacea, Gg root standardized extract could represent a relevant candidate for exploratory topical formulation studies. Therefore, the developed hydrogel was subjected to a comprehensive evaluation, including rheological characterization, release and skin permeation studies, antioxidant and antimicrobial activity against skin pathogens, cell viability, cytotoxicity assessment on HaCaT keratinocytes, and molecular target analysis via immunohistochemistry, as well as biocompatibility and angiogenesis testing using the chick chorioallantoic membrane (CAM) model.

2. Materials and Methods

2.1. Plant Material and Extract

As described in our previous work [21], dried Gg root was purchased from Laboratoarele Fares Bio Vital (Orăștie, Romania), a Romanian producer of plant-based remedies. The herbal product was also identified in the Pharmacognosy Department of "Victor Babeș", University

of Medicine and Pharmacy. A voucher specimen (23-GG-CD) was deposited at the Herbarium of the Faculty of Pharmacy (Department of Pharmacognosy-Phytotherapy), Timișoara.

After authentication, a mechanical grinder was used to grind the Gg roots. A methanolic extract was prepared, using 10 g of Gg powder and 100 mL of MeOH/H_2O (*v*/*v*-80/20), followed by 60 min of ultrasonication (50 °C, 59 KHz). The extract was subsequently filtered, concentrated by solvent evaporation, and finally dried.

2.2. Chemicals

Labrasol ALF (Caprylocaproyl Polyoxyl-8 glycerides) was acquired from Gattefossé (Saint-Priest Cedex, France). Xantural® 180 (xantan gum) was purchased from CP Kelco A Huber Company (Atlanta, GA, USA). Propylenglygol was obtained from Sigma-Aldrich (Budapest, Hungary). Purified water was used (Milli-Q system, Millipore, Milford, MA, USA). The cellulose acetate filter (Porafil membrane filter, cellulose acetate, pore diameter: 0.45 µm) was purchased from Macherey-Nagel GmbH & Co. KG (Düren, Germany).

Excised human skin was obtained from a Caucasian female patient by a routine plastic surgery procedure in the Albert Szent-Györgyi Health Center, Department of Dermatology and Allergology, University of Szeged. The measurements were performed with the approval of the Hungarian Medical Research Council (ETT-TUKEB, registration number: BMEÜ/2339-3/2022/EKU).

2.3. Preparation of Hydrogels

The hydrogel formulations were prepared as follows. For S1, xanthan gum was dispersed in half of the purified water and allowed to swell for 2 h. Meanwhile, the Gg extract at 2% (*w*/*w*) was dissolved in the remaining purified water, to which propylene glycol was added as a penetration enhancer. The extract solution was then gradually incorporated into the swollen polymer, and the mixture was stirred until a homogeneous hydrogel was obtained. A blank formulation (S1 blank) was prepared using the same procedure, but without the extract. For S2, the hydrogel was prepared in the same manner, substituting Labrasol ALF for propylene glycol as a penetration enhancer. The corresponding blank hydrogel (S2 blank) was obtained in the same way.

2.4. Rheological Measurements of Hydrogels

The rheological properties were studied with an Anton Paar Physica MCR302 Rheometer (Anton Paar, Graz, Austria). The measuring device was of the parallel plate type (diameter of 25 mm, gap height of 0.1 mm). The flow curves were recorded over the shear rate range from 0.1 to 100 and from 100 to 0.1 1/s at 25 °C.

2.5. Hydrogel Release and Permeation via Franz Diffusion Cells

In vitro release tests (IVRT) and in vitro permeation tests (IVPT) were carried out based on EMA guidelines [25]. A vertical Franz diffusion cell (Logan automated dry heat sampling system, Logan Instruments Corporation, Somerset, NJ, USA) was used for modeling the drug release (IVRT) and drug permeation (IVPT) of the drug from the formulation. In the case of IVRT, diffusion proceeds through a synthetic membrane, and in the case of IVPT, permeation proceeds through the heat-separated human epidermis (HSE). The heat-separation method was carried out in order to isolate the epidermis [26]. In the case of the donor phase, a quantity of about 300 mg of the sample was placed on the membrane (drug diffusion test—Porafil membrane filter, 0.45 µm pore-sized cellulose acetate) or the HSE. The receptor phase was a phosphate buffer solution (PBS pH 7.4 ± 0.15), which was kept at a temperature of 32 ± 0.5 °C. The duration of the IVRT was 6 h, and the sampling times were 0.5, 1, 2, 3, 4, 5, and 6 h. The duration of the IVPT was 24 h, and the sampling times were 0.5, 1, 2, 4, 6, 12, 18, and 24 h. The amount of released and

permeated extract was determined at a wavelength of 327 nm with a Thermo Scientific Evolution 201 spectrometer using the Thermo Insight v1.4.40 software package (Thermo Fisher Science, Waltham, MA, USA). Measurements were also performed with a drug-free formulation. Data were corrected with the data of drug-free formulations in all cases. Five parallel examinations were carried out (n = 5). The results were calculated as means ± SD. In the case of IVRT, the drug release rate was calculated from the slope of the cumulative amount of active substance (μg/cm^2) released versus the square root of time (h). In the case of IVPT, the permeation profiles of dermal formulations were obtained. The flux was the slope of the cumulative amounts of extract (μg/cm^2) permeated versus time (h) profiles.

2.6. Evaluation of the Antioxidant Activity

The antioxidant potential of the hydrogels was assessed using three complementary assays: the Ferric Reducing Antioxidant Power (FRAP) assay, the DPPH radical scavenging assay, and ABTS [2,2′-azinobis-(3-ethyl-benzothiazoline-6-sulfonic acid)].

Radical scavenging activity using the DPPH assay

The DPPH (1,1-diphenyl-2-picrylhydrazyl) assay was conducted according to the method of Brand-Williams et al. [27] with some modifications. Briefly, 0.1 mL of sample was added to 2.9 mL of freshly prepared 0.09 mM DPPH in methanol. The mixture was vortexed and incubated in the dark at room temperature for 2 h. The decrease in absorbance was measured at 515 nm using a Jasco V 530 UV-Vis spectrophotometer (ABL&E-JASCO, Wien, Austria). Trolox was used as an antioxidant reference compound. The calibration curve (y = 81.8044x + 0.9689, R^2 = 0.9982) was obtained using standard solutions in the range 0.1–0.6 mmol/L Trolox. The results were expressed as millimolar (mM) Trolox equivalents (TE).

Reducing activity through the FRAP Assay

In addition to the DPPH radical scavenging assay, the antioxidant potential of the hydrogels was further evaluated using the Ferric Reducing Antioxidant Power (FRAP) assay, as described by Benzie and Strain [28], with slight modifications. The FRAP reagent was prepared by mixing sodium acetate buffer (300 mM, pH 3.6), TPTZ solution (10 mM in 40 mM HCl), and $FeCl_3$ solution (20 mM) in a 10:1:1 ($v/v/v$) ratio. The resulting mixture was diluted with two volumes of double-distilled water and then incubated at 37 °C for 30 min. A total of 2.9 mL of the FRAP reagent was mixed with 0.1 mL of the sample solution and incubated in the dark at room temperature for 2 h. The absorbance was measured at 593 nm using a Jasco V 530 UV-Vis spectrophotometer (ABL&E-JASCO, Wien, Austria). A calibration curve (y = 1.4654x + 0.4140, R^2 = 0.9998) was obtained using different concentrations of Trolox in the range 0.1–0.6 mmol/L. The antioxidant activity was expressed as millimolar (mM) Trolox equivalents (TE).

ABTS assay

The ABTS [2,2′-azinobis-(3-ethyl-benzothiazoline-6-sulfonic acid)] assay was performed according to the method of Ozgen et al. [29]. The ABTS•$^+$ radical was generated by reacting 7 mmol/L ABTS with 2.45 mmol/L potassium persulfate in sodium acetate buffer (pH 4.5). The resulting dark blue-green solution was incubated in the dark at room temperature for 16–18 h, and subsequently diluted to achieve an absorbance value of ~1.0 at 734 nm. A total fo 2.9 mL of the ABTS solution was mixed with 0.1 mL of each sample and incubated in the dark at room temperature for 2 h. The decrease in absorbance was recorded at 734 nm using a Jasco V 530 UV-Vis spectrophotometer (ABL&E-JASCO, Wien, Austria). A calibration curve (y = 95.3731x + 1.7191, R^2 = 0.9993) was obtained using Trolox standard solutions in the concentration range of 0.1–0.6 mmol/L. The antioxidant activity was expressed as millimolar (mM) Trolox equivalents (TE).

All antioxidant analyses were conducted in triplicate (n = 3).

2.7. In Vitro Antimicrobial Evaluation

The antibacterial activity of hydrogels containing Gg extract was tested against ATCC bacterial strains obtained from Microbiologics (Enghien-les-Bains France). The tested strains included: *Streptococcus pyogenes* ATCC 19615, Staphylococcus aureus ATCC 25923, *Staphylococcus aureus* ATCC 29213, and *Cutibacterium acnes* ATCC 11827.

Antimicrobial activity was evaluated using the agar dilution method, adapted according to guidelines from both the European Committee on Antimicrobial Susceptibility Testing [30] and the Clinical and Laboratory Standards Institute [31]. A series of agar plates using different media were chosen, depending on the bacterial requirements: Mueller Hinton agar; Mueller Hinton agar supplemented with 5% horse blood and β-NAD; Mueller Hinton agar containing 5% sheep blood; Fastidious Anaerobe Agar with 5% horse blood; and supplemented Brucella agar. Each plate contained the test compounds at increasing concentrations prepared by doubling dilution (100, 50, 25, 12.5, 6.25, and 3.12 µg/mL).

A suspension of the microorganism was prepared in 0.85% saline to equal the turbidity of a 0.5 McFarland (except for *C. acnes*, which was adjusted to 1 McFarland), and 1 µL of this suspension was placed on each of the series of plates with increasing concentrations of the extracts, using a sterile loop. The plates were incubated at 35 ± 2 °C for 24 h under either ambient air or anaerobic conditions (AnaeroGen, ThermoScientific, Waltham, MA, USA). The minimum inhibitory concentration (MIC) was defined as the lowest concentration of evaluated samples at which complete inhibition of microorganism occurred. Antimicrobial determinations were performed in triplicate (n = 3).

2.8. Cell Line and Cell Culture Conditions

The in vitro model employed in the current study was composed by human immortalized keratinocytes–HaCaT cells (HaCaT: CLS 300493 (CLS Cell Lines Service GmbH (300493, Eppelheim, Germany)) in order to evaluate the biological profile of the two different samples of Gg-based gels (S1 and S2). The immortalized keratinocyte cell line was cultured using the following reagents: DMEM high glucose (4.5 g/L) media, with 15 mM HEPES, and 2 mM L-glutamine (Sigma-Aldrich, Munich, Germany) supplemented with 10% heat-inactivated fetal bovine serum and 1% antibiotic mixture of 100 U/mL penicillin: 100 µg/mL streptomycin, to avoid any possible fungal or bacteriological infections. During the entire period of the experiment, the specific sterile working conditions with cell cultures were respected, using the biosafety cabinet Ehret V-130 (Ehret GmbH & Co KG, Emmendingen, Germany).

2.9. Cell Viability Evaluation by Means of MTT Colorimetric Assay

The biological activity induced by the test sample of Gg-based gels (S1 and S2) and their corresponding blank gels (S1_blank and S2_blank) on human immortalized keratinocyte (HaCaT) viability was assessed by means of a 3-(4,5-dimethylthiazol-2-yl)-2,5-diphenyl-2H-tetrazolium bromide (MTT) colorimetric test, as previously described [32]. In brief, a density of 1×10^4 cells/well was cultured onto 96-well culture plates and incubated until a confluence of 70–80% was reached. Afterwards, the cells were stimulated for 72 h with four different concentrations (25, 50, 100, and 200 µg/mL) of test samples (S1 and S2, and their corresponding blank samples, S1_blank and S2_blank). As control cells, HaCaT cells were used, however they were treated only with the culture medium for the same time interval (72 h). To quantify the cell viability rate, the absorbance of the 96-well plate was measured spectrophotometrically at 560 nm wavelength using the microplate reader (GloMax Discover, Promega, Madison, WI, USA).

2.10. Neutral Red (NR) Assay

To provide complementary information to the one obtained by the MTT proliferation assay, the NR method was also performed, in order to quantify the sample cytotoxicity rate. The principle of this method is based on the quantification of viable cells through staining the lysosomes of the living cells with the NR chromophore. The uptake of the dye is realized via active transport; thus, the non-living cells are not able to incorporate the NR reagent. Therefore, the living cells can release the NR dye under acidified conditions, and the intensity of the dye can be further correlated with the number of living cells, and thus, to drug-induced cytotoxicity.

In brief, the protocol consisted of treating the cells with four concentrations (25, 50, 100, and 200 µg/mL) of test samples for 72 h. Afterwards, 10 µL of 0.33% NR solution was added in each well for at least 3 h and further incubated. At the end of the incubation period, the medium was removed and the cells were quickly washed with 50 µL NR assay fixative solution, following a solubilisation step using NR assay solubilization solution (100 µL/well).

2.11. Lactate Dehydrogenase (LDH) Release Method

The LDH method assesses the release of the intracellular lactate dehydrogenase in the extracellular environment following the cellular membrane impairment, therefore this method provides information related to necrosis-like events [33]. Thus, the LDH test was employed in the current study to evaluate the cytotoxicity necrosis-related events that occurred after exposure of the HaCaT cells to the test samples (S1 and S2, and their corresponding blank samples, S1_blank and S2_blank) for a period of 72 h. The protocol was performed in good agreement with the instructions included in the Pierce LDH cytotoxicity assay kit provided by the manufacturer (Thermo Fisher Scientific, Boston, MA, USA), as already described in detail in our previous studies [34].

All cell-based assays were performed in triplicate (n = 3).

2.12. In Ovo Assessment

General CAM method

The chorioallantoic membrane (CAM) assay was employed as an in vivo model to evaluate the biological effects of the LR hydrogel on the developing vascularized membrane of fertilized hen eggs (*Gallus gallus domesticus*). Eggs were sterilized with 70% ethanol and incubated at 37 °C with 50% relative humidity. On embryonic day 3 (EDD 3), 3–4 mL of albumen was gently removed to create space for membrane development, and a window was opened on the eggshell on EDD 4. Throughout the incubation period, the CAM was inspected daily using a stereomicroscope (ZEISS SteREO Discovery.V8, Göttingen, Germany), and images were acquired and analyzed with an Axiocam 105 color camera, while image processing was conducted using the dedicated AxioVision SE64. Rel. 4.9.1 software (ZEISS, Göttingen, Germany), ImageJ (ImageJ Version 1.50e, https://imagej.nih.gov/ij/index.html, accessed on 21 January 2025), and GIMP software (GIMP v 2.8, https://www.gimp.org/, accessed on 21 January 2025). Images were acquired both prior to and five minutes following the application of the tested samples.

Irritability evaluation by the HET-CAM Assay

The irritability potential of the LR hydrogel was assessed using a modified Hen's Egg Test—Chorioallantoic Membrane (HET-CAM) assay, an established alternative method for evaluating irritation on mucous membranes and skin, in compliance with ICCVAM recommendations [35,36]. Fertilized eggs were incubated until EDD 9, at which point 0.3 mL of hydrogels S1 and S2 and their corresponding blank were applied directly onto the CAM under stereomicroscope guidance. Sodium lauryl sulfate (SLS) 1% was used as

a positive control, and distilled water as a negative control. The CAM was monitored for 300 s for irritation signs including hemorrhage, vascular lysis, and coagulation. The time of onset (in seconds) for each parameter was recorded, and an irritation score (IS) was calculated as follows:

$$IS = 5 \times \left[\frac{301 - \text{Sec H}}{300}\right] + 7 \times \left[\frac{301 - \text{Sec L}}{300}\right] + 9 \times \left[\frac{301 - \text{Sec C}}{300}\right]$$

where IS = irritation score, Sec H is the onset (in seconds) of hemorrhagic reactions on the membrane, Sec L is onset (in seconds) of lysis of the vessel on the membrane, and Sec C is the onset (in seconds) of the formation of coagulation on the membrane. Irritation scores were then compared to a grading system established by Luepke: 0–0.9 indicates non-irritation, 1–4.9 indicates weak irritation, 5–8.9 indicates moderate irritation, and 9–21 indicates strong irritation [37], allowing a standardized classification of the tested samples according to their irritative potential. Experiments were performed in triplicate (n = 3).

2.13. Histological and Immunohistochemical Analysis

To evaluate the morphological changes and molecular markers associated with apoptosis and angiogenesis, a cell block technique was employed. After 72 h of exposure to the treatments (S1 and S2, and blanks at concentrations of 25, 50, 100, and 200 μg/mL), HaCaT cells were harvested and centrifuged, and the resulting pellets were fixed in 10% neutral buffered formalin. The cell pellets were processed as cytoblocks following a standard pathology protocol, embedded in paraffin, and sectioned.

For histological assessment, sections were stained with Hematoxylin-Eosin (HE) to visualize cellular architecture and cytoplasmic changes. Immunohistochemical (IHC) staining was performed to detect the expression of CD44 (cell adhesion), VEGF (angiogenesis), and Caspase-3 (apoptosis). The staining procedure was automated using the Autostainer Link 48 system (Dako, Agilent, CA, USA). The protocol utilized the EnVision FLEX visualization system (https://www.agilent.com/en/product/immunohistochemistry/visualization-systems/envision-flex-systems, accessed on 10 September 2025) with high-pH target retrieval.

The following primary antibodies were used: Anti-CD44 Monoclonal Mouse Anti-Human (Clone 156-3C11, ready-to-use); Anti-VEGF Monoclonal Mouse Anti-Human (Clone VG1, ready-to-use); and Monoclonal Mouse Anti-Human Anti-Caspase 3 (Polyclonal Rabbit, ready-to-use), from Agilent Technologies, Santa Clara, CA, USA. Signal detection was achieved using the PolyVue™ Plus Mouse/Rabbit HRP/DAB Kit (Diagnostic, BioSystems, Pleasanton, CA, USA). The slides were counterstained with hematoxylin, dehydrated, and mounted for microscopic evaluation (performed by a board-certified pathologist: E.G.O).

Histological and IHC assessment was performed in a qualitative manner, focusing on the distribution patterns and intensity of signal expression across the cell blocks. This approach was selected to provide a descriptive safety profile and to identify potential dose-dependent trends in marker expression.

Statistical Analysis

GraphPad Prism 9 version 9.3 (GraphPad Software, San Diego, CA, USA) was employed for data representation and statistical analysis. The results are presented as mean values ± standard deviation (SD). One-way ANOVA followed by Dunnett's post-test was used to obtain the statistical differences as indicated in the corresponding figure legends.

3. Results

Our previous study on this topic consisted of a thorough phytochemical analysis of the Gg root methanolic extract [21]. As it was shown in that study [21] the follow-

ing compounds were identified: glycyrrhizin, liquiritin, liquiritigenin-apiosyl-glucoside, apigenin-rutinoside, liquiritigenin, apigenin- methylether-glucoside, luteolin-glucoside, luteolin-rutinoside, apigenin-apiosyl-glucoside. Moreover, the methanolic extract elicited antioxidant activity as shown by DPPH and ABTS assays and lack of toxicity as shown by metal content analysis conducted by atomic absorption spectroscopy assay [21]. Following this previous study, two different extract-based hydrogels were formulated, to evaluate their proprieties for potential future use in topical applications, as a natural approach for the management of rosacea.

3.1. Rheological Properties of Hydrogels

Rheological characteristics are important properties of colloid systems, related to the nature and extent of the intermolecular interactions and the entanglements of the polymer chains. Figure 1 shows the flow curves of the blank hydrogels and hydrogels containing Gg extract. In the flow curves, slight thixotropy was observed in the case of all preparations. The extract content increased the shear stress of the system, which means that the extract increased the viscosity of the hydrogel. It can be assumed that there are interactions between the active substance and the polymer chains. The penetration enhancers did not influence the parameters significantly. The rheological measurements showed that the formulations are suitable for dermal use.

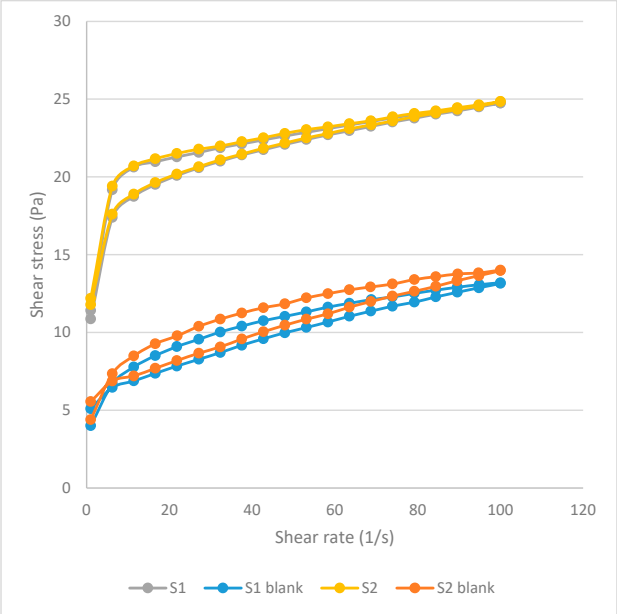


Figure 1. Flow curves of hydrogels S1 and S2 and their corresponding blank formulations at 25 °C.

3.2. Hydrogel Release and Permeation Profiles of Hydrogels

In this study, Gg extract was formulated in hydrogel preparations, and the investigation of biopharmaceutical properties was carried out using a vertical Franz diffusion cell system. After 6 h, the cumulative amounts of extract released were 2923 μg/cm^2 for formulation S1 and 3312 μg/cm^2 for S2, corresponding to 32.15% and 33.05% of the total extract content in the donor phase, respectively. The release rates, calculated from the linear portions of the release curves, were 1204.3 μg/cm^2/h (R^2 = 0.9952) for S1 and 1372.4 μg/cm^2/h (R^2 = 0.9943) for S2 (Figure 2).

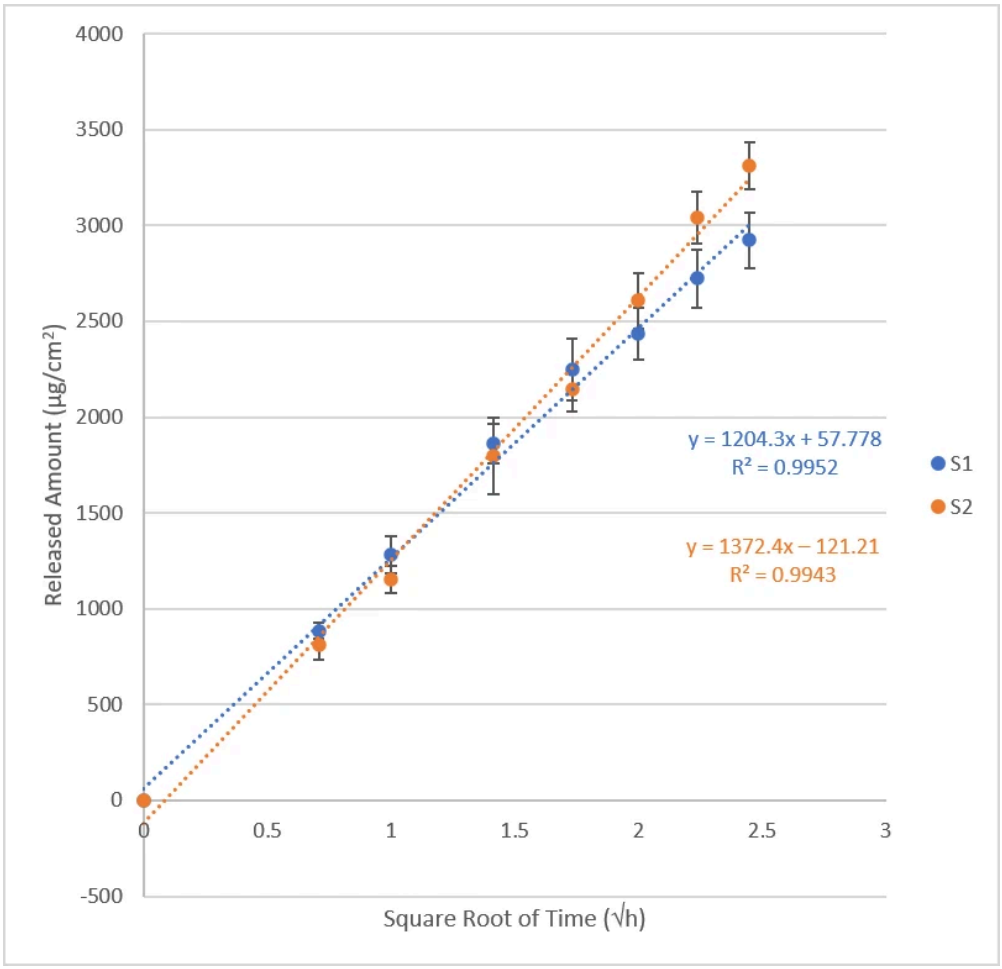


Figure 2. Drug release rate from hydrogels (IVRT).

In the permeation test across the human epidermis, the cumulative amounts of extract that permeated after 24 h were 204.7 µg/cm^2 (S1) and 245.4 µg/cm^2 (S2), with corresponding fluxes of 7.357 µg/cm^2/h (R^2 = 0.9837) and 9.305 µg/cm^2/h (R^2 = 0.9707) (Figure 3).

The in vitro release test (IVRT) was used to evaluate the rate and extent of diffusion of active ingredients from the formulations. The results within this study show a gradual release of Gg extract from both hydrogels (approximately 32–33% within 6 h), with no statistically significant difference between S1 and S2. Due to the barrier function of the human epidermis, the amount of permeated extract was much lower than in the case of IVRT. However, the permeation through the biological membrane is continuous during the detected period. The flux of the S2 formulation was slightly higher, but no significant difference was found. It can be said that IVRT is specific to the formulation, while in vitro–in vivo correlation is expected for IVPT.

Based on the above-mentioned investigations, it can be observed that xanthan gum, used as a gelling agent, hindered the drug release, as well as causing a decrease in the ability of entrapping the drug within the gel.

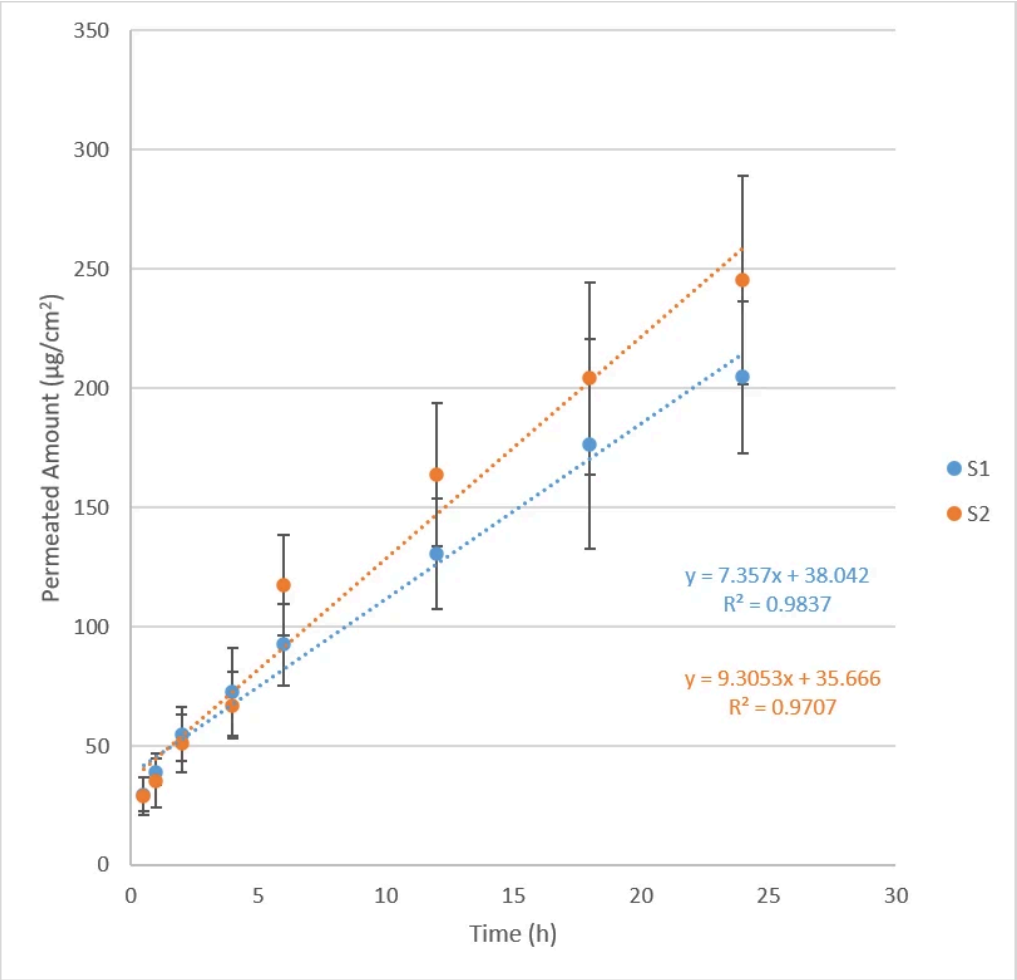


Figure 3. Drug permeation through the human epidermis (IVPT).

3.3. Antioxidant Activity of the Hydrogel Formulations

In our previous study [21], the antioxidant activity of the methanolic Gg extract was assessed by the DPPH assay, providing a baseline of its free-radical scavenging capacity. In the present work, to verify whether these properties were maintained after formulation and to capture a broader mechanistic profile, the hydrogels were evaluated by three complementary assays—DPPH, ABTS, and FRAP—reflecting hydrogen-donating, total radical-quenching, and ferric-reducing activities, respectively.

Both extract-containing hydrogel formulations (S1 and S2) exhibited significantly higher antioxidant activities compared with their respective blanks ($p < 0.05$), confirming that the observed effects originated from the incorporated Gg extract. At the tested concentration of 50 mg gel/mL, corresponding to 1 mg extract/mL of sample, the formulations displayed marked activity across all three assays (Table 1). For S1, the antioxidant capacities were 0.275 ± 0.008 mM TE (DPPH), 0.530 ± 0.016 mM TE (ABTS), and 0.198 ± 0.004 mM TE (FRAP); for S2, the respective values were 0.283 ± 0.012 mM TE, 0.509 ± 0.004 mM TE, and 0.203 ± 0.008 mM TE. The blank hydrogels showed negligible activity (≤0.04 mM TE in all assays).

Table 1. Antioxidant activity evaluated for the hydrogels S1 and S2, containing Gg extract.

Nr.	Samples (50 mg/mL)	Antioxidant Activity (mM TE)		
		DPPH	ABTS	FRAP
1	S1 blank	0.040 ± 0.002	0.025 ± 0.002	0.011 ± 0.001
2	S1	0.275 ± 0.008	0.530 ± 0.016	0.198 ± 0.004
3	S2 blank	0.034 ± 0.003	0.024 ± 0.001	0.011 ± 0.001
4	S2	0.283 ± 0.012	0.509 ± 0.004	0.203 ± 0.008

Considering the 2%(*w*/*w*) extract loading, these values correspond to approximately 0.2–0.5 µmol TE/mg extract (≈200–530 µmol TE/g extract), indicating a high level of antioxidant efficiency retained within the semisolid matrix. Among the assays, ABTS values were highest, making this method particularly sensitive to the polyphenolic and flavonoid components present in Gg extracts, followed by DPPH and FRAP, reflecting differences in radical type, solvent polarity, and mechanism of action—with ABTS being more responsive to both hydrophilic and lipophilic antioxidants, DPPH favoring moderately polar radicals, and FRAP reflecting purely electron-transfer capacity under acidic conditions.

3.4. Antimicrobial Analysis

The antimicrobial activity of both gel samples (S1 and S2) and blanks (S1B and S2B) was assessed against four bacterial strains involved directly or indirectly in the occurrence of rosacea: *Streptococcus pyogenes* (ATCC 19615), *Cutibacterium acnes* (ATCC 11827), and two strains of *Staphylococcus aureus* (ATCC 25923 and ATCC 29213).

The results showed that two of the strains (*Streptococcus pyogenes* and *Cutibacterium acnes*) were sensitive to the tested Gg extract gels, with MIC values of 6.25–12.5 mg/mL. On the other hand, both *Staphylococcus aureus* strains were less susceptible to the Gg gels, showing a MIC value of 50 mg/mL (Table 2).

Table 2. Antibacterial activity of Gg gel formulation, as the minimal inhibitory concentration (MIC), for selected strains after incubation with extract.

Bacterial Strain	MIC (mg/mL)			
	S1	S1 Blank	S2	S2 Blank
Streptococcus pyogenes ATCC 19615	12.5	–	6.25	–
Staphylococcus aureus ATCC 25923	50	–	50	–
Staphylococcus aureus ATCC 29213	50	–	50	–
Cutibacterium acnes ATCC 11827	12.5	–	6.25	–

3.5. Cell Viability Assessment Through MTT Colorimetric Test

The cell viability of human immortalized keratinocytes (HaCaT) exposed to the Gg hydrogel formulations and their corresponding blanks was evaluated by the MTT test to determine metabolic activity and biocompatibility. The viability of HaCaT cells following exposure to the Gg hydrogels (S1 and S2) and their corresponding blanks is shown in Figure 4. Overall, HaCaT cells were slightly more sensitive to S1, with viability decreasing below 80% at 200 µg/mL. In contrast, exposure to S2 maintained cell viability above 84% at the same concentration. Both blank formulations preserved high cell viability (>86.5%), confirming good in vitro biocompatibility of the gel matrix.

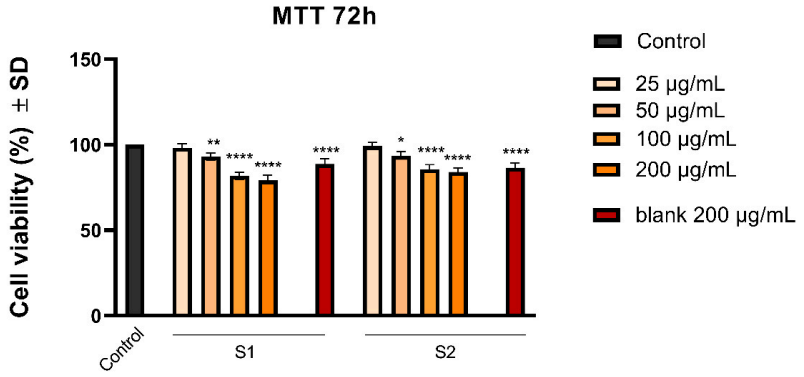


Figure 4. Cell viability percentages of HaCaT cells exposed to S1 and S2 and their blanks for 72 h. Cell viability percentages were normalized to control cells (cells treated with culture medium). Data are presented as mean values ± standard deviation (SD). One-way ANOVA analysis was applied to determine the statistical differences followed by Dunnett's comparisons test (* $p < 0.1$; ** $p < 0.01$; **** $p < 0.0001$).

3.6. Cytotoxicity Rate via NR Method

Sample-induced cytotoxicity by assessing the lysosome impairment was realized by means of the NR assay. The results obtained are presented in Figure 5, showing that at concentrations of 25 µg/mL and 50 µg/mL of S1 and S2, only minimal cytotoxic events occurred, whereas at higher concentrations of 200 µg/mL, the cytotoxicity percentage increased above 21% for both the S1 and S2 gels.

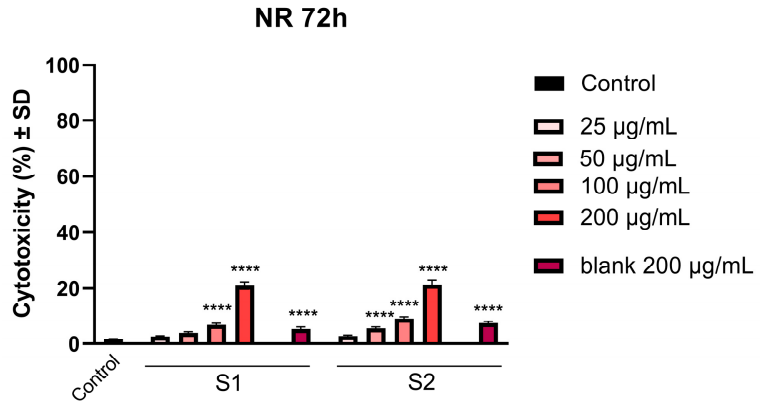


Figure 5. Cytotoxicity rate in HaCaT cells exposed to S1 and S2 and their blanks for 72 h. Data are presented as mean values ± standard deviation (SD). One-way ANOVA analysis was applied to determine the statistical differences followed by Dunnett's comparisons test (**** $p < 0.0001$ versus control cells).

3.7. Lactate Dehydrogenase Quantification for Necrosis-Related Events

Figure 6 presents the LDH leakage percentage resulting from the loss of the cell membrane integrity in immortalized human keratinocytes (HaCaT) after exposure to Gg-based gels (S1 and S2) and their corresponding blank gels (S1_blank and S2_blank) for an interval of 72 h. The results obtained present the same pattern as the ones revealed by the NR test; however, at low concentrations (25 and 50 µg/mL), a smaller population of cells showed necrotic aspects through cell membrane destruction compared to the damage of cellular digestion through lysosome impairment, as the LDH released rate presents a few percent less than those recorded via the NR test, especially for the S2 formulation. Nevertheless, at the highest concentration of 200 µg/mL, the S1 gel induced a percentage of 24.7%, while the S2 gel induced a necrosis-related rate of 15.8% when applied for an interval of 72 h.

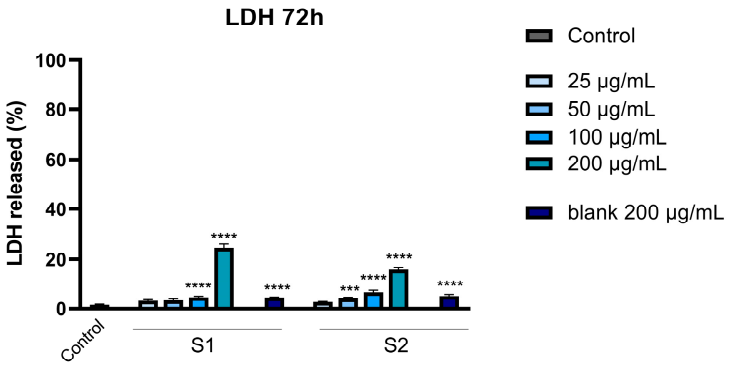


Figure 6. LDH release ratio of HaCaT cells after exposure to S1 and S2 and their blanks for 72 h. One-way ANOVA analysis was applied to determine the statistical differences, followed by Dunnett's multiple comparisons test (*** $p < 0.001$; and **** $p < 0.0001$ versus control cells).

3.8. Biocompatibility and Irritation Assessment on the Chorioallantoic Membrane (CAM)

Biocompatibility of the hydrogels was evaluated using the HET-CAM assay on the chorioallantoic membrane (CAM). No signs of irritation were observed following hydrogel application, with no evidence of hemorrhage, vascular lysis, or coagulation throughout the observation period. These findings were comparable to the negative control (distilled water), indicating excellent tolerability. In contrast, the positive control, sodium lauryl sulfate (SLS), induced a pronounced irritative response characterized by an IS of 17.19, confirming the assay's sensitivity (Table 3, Figure 7). Overall, the hydrogels demonstrated a favorable biocompatibility profile with no irritation risk when applied topically.

Table 3. Irritation scores and observed effects of the two hydrogels, S1 and S2, and their blanks in the HET-CAM assay.

Sample	Irritation Score	Effect Type
SLS (positive control)	17.19 ± 0.24	strong irritant
H_2O (negative control)	0 ± 0	non-irritant
S1 blank	0 ± 0	non-irritant
S2 blank	0 ± 0	non-irritant
S1	0 ± 0	non-irritant
S2	0 ± 0	non-irritant

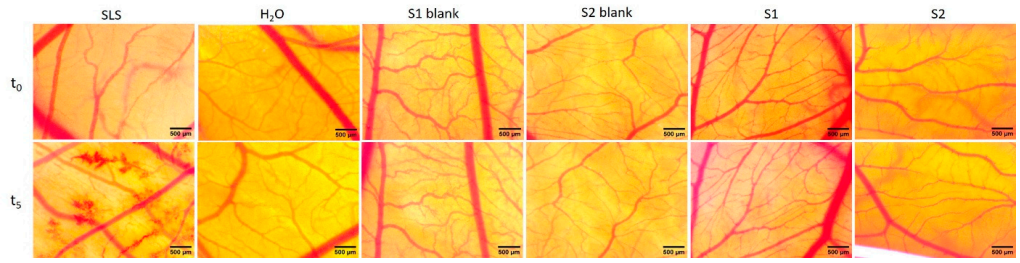


Figure 7. HET-CAM evaluation of hydrogel irritation potential. The in ovo stereomicroscopic images from the HET-CAM assay show the CAMs at initial contact (t_0) and after 300 s (t_5) following application of S1 and S2 and their blanks. Scale bars represent 500 µm.

3.9. Angiogenic Responses Using the CAM Model

To evaluate the impact of the hydrogels on vascular development, the angiogenic response on the chorioallantoic membrane (CAM) was monitored following application of the formulations from embryonic day 7 (EDD 7). Angiogenesis proceeded normally during

the first 24 h following application from EDD 7. However, both hydrogels containing licorice extract exhibited a noticeable reduction in the formation of small blood vessels and a thinning of the existing capillaries. These anti-angiogenic effects were more pronounced in the S2 formulation, becoming especially evident 48 h after application.

Visible differences were observed between the extract-containing hydrogels and the blank samples, with intense angiogenesis persisting in the blanks even 48 h after application. In contrast, the hydrogels containing licorice extract exhibited a gradual modulation of angiogenic activity over this period, indicating prolonged biological effects associated with the active constituents (Figure 8). Meanwhile, the blank formulations showed no influence on vascular development, confirming their inert nature in this model.

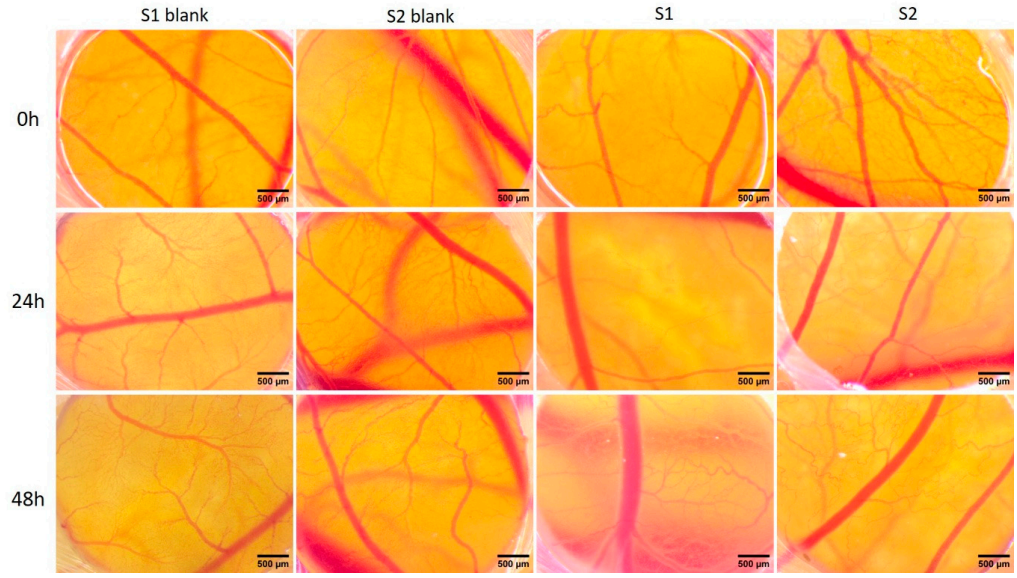


Figure 8. Effects of extract-containing hydrogels on normal CAM angiogenesis: stereomicroscopic images comparing angiogenic responses with blank samples. Scale bars represent 500 µm.

3.10. Histological and Immunohistochemical Assessment

The histological analysis (HE) of the HaCaT cytoblocks revealed distinct, dose-dependent morphological changes between the two formulations. For formulation S1 (Figure 9), viable keratinocyte aggregates with preserved nucleocytoplasmic ratios were observed at concentrations between 25 and 100 µg/mL. However, at concentrations of 200 µg/mL, distinct cytoplasmic eosinophilia was noted, indicative of intracellular acidification and the onset of apoptotic processes.

Regarding the technical integrity of the samples, a specific limitation was encountered. While the HE staining for the blank controls demonstrated normal cellular morphology with no nucleocytoplasmic alterations, the corresponding cell blocks were lost during subsequent processing, precluding IHC analysis for the control group.

In contrast, formulation S2 demonstrated a superior safety profile (Figure 10). While cytoplasmic eosinophilia was also observed at a higher concentration (200 µg/mL), the cells maintained sufficient viability and material integrity to allow for complete IHC analysis.

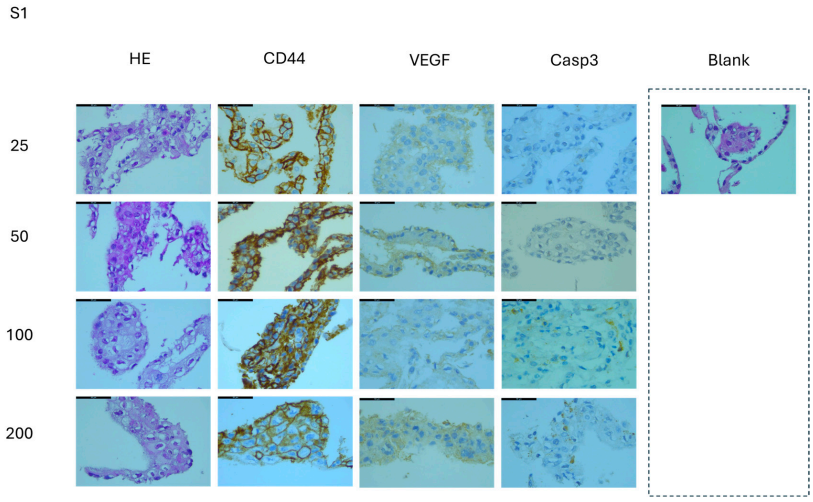


Figure 9. Histological and IHC analysis of HaCaT cell blocks following 72 h exposure to S1 hydrogel at concentrations of 25, 50, 100, and 200 μg/mL. HE staining reveals viable cell aggregates with preserved nucleocytoplasmic ratios at 25–100 μg/mL, shifting to distinct cytoplasmic eosinophilia at 200 μg/mL. IHC panels demonstrate: CD44 (membrane staining, brown) retaining high intensity at lower concentrations but showing reduced intensity and loss of intercellular adhesion at 200 μg/mL; VEGF displaying low-to-moderate cytoplasmic expression without evident membrane accentuation, consistent with an anti-angiogenic profile; and Caspase-3 showing positive expression (brown chromogen) at concentrations ≥ 100 μg/mL, indicating the activation of apoptotic pathways. The blank control is presented with HE staining only, as the cell block material for this group was lost during processing, precluding IHC analysis; All photomicrographs were captured using a 63× Leica dry objective (scale bar: 50 μm).

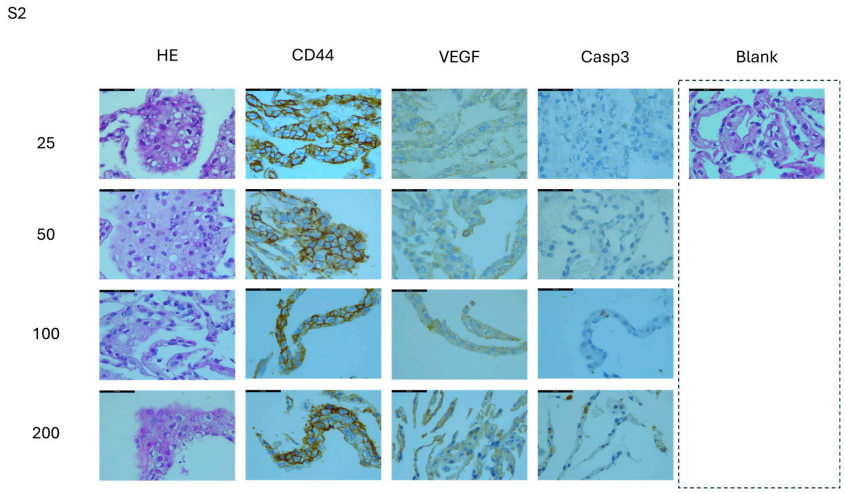


Figure 10. Histological and immunohistochemical analysis of HaCaT cell blocks following 72 h exposure to S2 hydrogel at concentrations of 25, 50, 100, and 200 μg/mL. HE staining demonstrates viable keratinocyte aggregates across all concentrations; while cytoplasmic eosinophilia increases at 200 μg/mL, cellular integrity and viability are better preserved compared to the S1 formulation. IHC panels reveal: CD44 (membrane staining, brown) maintaining relatively high intensity and continuous membrane expression even at the maximum concentration of 200 μg/mL, indicative of superior preservation of cell adhesion; VEGF exhibiting moderate-to-low cytoplasmic expression without membrane accentuation, supporting an anti-angiogenic mechanism; and Caspase-3 showing positive expression (brown chromogen) at concentrations ≥ 100 μg/mL, confirming a controlled apoptotic response rather than necrosis. The Blank control is represented by HE staining only, as the corresponding cell block material for the control group was lost during processing; All photomicrographs were captured using a 63× Leica dry objective (scale bar: 50 μm).

Immunohistochemical staining revealed the following expression patterns:

CD44: Expression was preserved with high membrane intensity (brown chromogen) at lower concentrations (25–100 μg/mL) for both formulations. In S1-treated cells, a loss of intensity and intra-cellular adhesion was noted at 200 μg/mL. Conversely, S2-treated cells maintained relatively intense CD44 expression, even at 200 μg/mL.

VEGF: Both formulations induced a moderate-to-low expression of VEGF. Notably, there was a lack of evident membrane intensity across all concentrations. In the context of non-stimulated keratinocytes, this expression profile suggests that the formulations do not induce pro-angiogenic signaling, maintaining a baseline phenotype consistent with the anti-angiogenic potential observed in the CAM assay.

Caspase-3: Expression (brown chromogen) was absent at low concentrations, but became visible at concentrations of 100 μg/mL and higher. This positivity signifies a shift towards a controlled apoptotic turnover at higher concentrations, corroborating the eosinophilic cytoplasmic changes observed in HE staining.

4. Discussion

Rosacea is estimated to affect over 5% of the world population [38], significantly contributing to a number of psychological side effects [39]. Given that the physiopathology of this skin condition is still unclear and the medication used to treat it has not changed nor improved too much over the years, it feels difficult for many rosacea patients to find a steady course of treatment. The fact that topical metronidazole or azelaic acid have been used for a long time, with relatively good results [6], gives this medication good odds, but it is insufficient, especially in a world where the aggravating factors become more present. Laser-based therapies, particularly pulsed dye laser (PDL), have also shown efficacy in reducing erythema and telangiectasia in rosacea [40]. However, there is still room for development in regard to the optimal care and treatment for rosacea-affected skin. Even though the main cause of developing rosacea is yet uncertain, research continues to uncover some major pathways that involve the skin immune system, mast cells, and other neurovascular abnormalities. These situations affect skin barrier function, permeability of the vascular system, hydration, the microbiome, and even pH values [41].

There is now increasing evidence that rosacea is a chronic inflammatory skin disease, characterized by vascular and neurovascular changes, dysregulation of innate and adaptive immune responses, increased density of Demodex mites, enhanced oxidative stress, and impairment of the skin barrier [42]. Taking this into consideration, it seems important that new topical treatment is added to the existing one, so that it can address at least some of these contributing factors. Gg has been used to treat various diseases for over 3000 years. In Chinese traditional medicine, it was used, among others, to treat skin conditions like psoriasis, eczema, and acne. However, it is only more recently that studies revealed part of its phytochemical composition and how these phytochemicals give Gg the ability to be useful in the management of these skin conditions [43,44]. Numerous studies have demonstrated that its bioactive components—particularly triterpenes like glycyrrhizin and glycyrrhetinic acid, and a variety of flavonoids such as echinatin, glabridin, isoliquiritigenin, and licochalcones A through E, as well as licoricidin and licorisoflavan A—exhibit notable anti-inflammatory effects [45,46]. Importantly, several bioactive compounds likely underlying the antioxidant, antimicrobial, and anti-angiogenic effects observed in this study were previously identified and quantitatively characterized in the same methanolic Gg root extract by our group using HPLC-DAD-ESI+, with glycyrrhizin as the major constituent (13.927 mg/g dry extract), accompanied by abundant flavonoids including liquiritin, liquiritigenin, liquiritigenin-apiosyl-glucoside, apigenin-rutinoside, luteolin, and apigenin-based glycosides [21]. Extensive pharmacological evaluations have validated these compounds

as potent antioxidant, anti-inflammatory, and antibacterial compounds. By targeting these multiple pathways, these bioactives offer a multifaceted approach to managing complex inflammatory conditions [47–49]. Glycyrrhizin, in particular, has an action profile similar to that of glucocorticoids and mineralocorticoids, capable of suppressing inflammatory mediators and supporting the healing of both gastric and oral ulcers [46]. Additionally, both glycyrrhizin and 18β-glycyrrhetinic acid have been identified as effective inhibitors of key pro-inflammatory factors, including cyclooxygenase-2 (COX-2), high-mobility group protein 1 (HMGP1), inducible nitric oxide synthase (iNOS), interleukins IL-6 and IL-10, tumor necrosis factor-α (TNF-α), transforming growth factor-beta (TGF-β), prostaglandin E2 (PGE2), myeloperoxidase (MPO), and nuclear factor-kappa B (NF-κB) [46,50]. Moreover, in their study, Fatoki et al. [49] demonstrated that some of the active phytochemicals present in Gg (such as glycyrrhizin, liquiritin, isoliquiritin, liquiritin apioside, and glucoliquiritin apioside) possess good skin-permeability properties. Some of the preliminary results obtained from experiments evaluating the proprieties of Gg hydrogels were initially briefly described by Semenescu et al. [51].

Considering that rosacea has been described as an inflammatory skin disease, accompanied by vascular changes and skin microbiome dysbiosis, the properties of the Gg extract justify its exploration in preclinical topical formulations relevant to rosacea-prone skin. Effective management requires formulations that not only target microbial agents but also modulate inflammation, vascular changes, and ensure skin compatibility. In this context, evaluating the rheological properties of topical formulations is essential for optimizing application and patient compliance. Controlled release and permeation studies are crucial to ensure the adequate bioavailability of active compounds at the target site. Antimicrobial activity assessment addresses the role of skin-associated bacteria in disease exacerbation, while cytotoxicity testing on keratinocytes provides insight into the safety profile of the formulation on skin cells. Moreover, biocompatibility and irritation was investigated using alternative in vivo models such as the HET-CAM assay, which offers a sensitive platform to predict ocular and dermal tolerability. Finally, angiogenesis evaluation on the chorioallantoic membrane (CAM) relates directly to the vascular alterations seen in rosacea, allowing an understanding of the formulation's potential impact on pathological neovascularization. Together, these multidisciplinary analyses provide a comprehensive framework supporting further exploration in preclinical topical formulation studies.

4.1. Formulation

Because of their hydrophilic ability, hydrogels have the advantage of being able to entrap many of the herbal extracts, so they can be used as a medicinal delivery system [52]. The many useful proprieties of hydrogels in general [53], and particularly of xanthan gum, have been described previously [54]. Moreover, taking into consideration different studies on xanthan gum delivery systems, it seemed optimal that the concentration of xanthan gum gel used in this particular situation was 2% [55].

In this study, four hydrogels were prepared (S1, S1 blank, S2, and S2 blank), using the same concentration of xanthan gum (2%), and two different penetration enhancers: propylene glycol (S1) and Labrasol ALF (caprylocaproyl polyoxyl-8 glycerides, S2). All four of the gels were assessed for their rheological proprieties, and underwent in vitro release tests (IVRT), in vitro permeation tests (IVPT), and in vitro biocompatibility tests.

The rheological assessment showed that shear stress increased in the preparations containing the extract, which means that the extract increased the viscosity of the hydrogel. These results are similar to those obtained by Mees et al. in their study [56]. The addition of penetration enhancers did not produce significant changes in the evaluated parameters.

Rheological analysis confirmed that all formulations possess appropriate characteristics for dermal application.

IVRT results indicated a controlled release of the active compound from both hydrogels, with 32.15% and 33.05% of the initial extract load released over a period of 6 h. The release profiles demonstrated good linearity, confirming that the hydrogels provided a sustained and reproducible release pattern. Although S2 showed marginally higher release values, no statistically significant difference was observed between the formulations. This release behavior aligns with findings by Wang et al. [43], who reported the sustained release of flavonoid-rich plant extracts from hydrogel systems due to their hydrophilic matrix structure and the swelling-controlled diffusion mechanism.

IVPT results showed lower cumulative permeation through the human epidermis—204.7 μg/cm^2 for S1 and 245.4 μg/cm^2 for S2 over 24 h—a reflection of the well-documented barrier properties of the stratum corneum. Despite this, both formulations exhibited sustained permeation profiles, and high correlation coefficients (R^2 = 0.9837 for S1 and 0.9707 for S2), suggesting a continuous release and permeation process over the tested period. These results are in agreement with Armanini et al. [57], who observed limited but sustained percutaneous absorption of glycyrrhetinic acid from topical formulations, attributed to its relatively high molecular weight and lipophilicity.

While both S1 and S2 demonstrated acceptable performance, the slightly higher release and permeation values for S2 may be associated with differences in excipient composition, affecting the gel's microstructure and drug mobility. However, as the differences were not statistically significant, both formulations can be considered pharmaceutically equivalent in terms of release and permeation behavior. These results are consistent with prior literature and reinforce the relevance of Gg as a bioactive agent with potential applications in dermatology, especially for inflammatory skin conditions such as eczema, rosacea, and psoriasis.

4.2. Antioxidant Effect

As previously described, in the management of rosacea, it is crucial for topical preparations to exert antioxidant effects due to the significant role that oxidative stress plays in the pathophysiology of the disease. Patients with rosacea often exhibit elevated levels of reactive oxygen species (ROS) in the skin, which contribute to vascular dysfunction, inflammatory responses, and tissue damage. ROS can activate key signaling pathways, such as nuclear factor-kappa B (NF-κB), leading to the upregulation of pro-inflammatory cytokines and matrix metalloproteinases, thereby exacerbating skin inflammation and barrier disruption. Moreover, oxidative stress amplifies the abnormal innate immune responses observed in rosacea, further promoting the release of cathelicidins and other inflammatory mediators. Therefore, incorporating antioxidants into topical treatments can help neutralize ROS, reduce inflammation, and restore skin homeostasis, making them a valuable component in the comprehensive management of rosacea [49,58,59].

In our previous study [21], the methanolic extract of Gg roots showed high DPPH radical-scavenging capacity (79.29 ± 0.82% inhibition at 1000 μg/mL), comparable to ascorbic acid (85.47 ± 0.62% at 50 μg/mL). The present study demonstrates that these antioxidant properties are largely preserved following incorporation into hydrogel matrices, as reflected by DPPH, ABTS, and FRAP values of 0.20–0.53 mM TE. When expressed per extract content, these values correspond to approximately 200–530 μmol TE/g extract, which are substantially higher than those reported for methanolic extracts in solution (ABTS ≈ 117.6, DPPH ≈ 58.2, FRAP ≈ 23.9 μmol TE/g) by Babich et al. [19]. This indicates that the hydrogel system preserved, and possibly enhanced, the apparent redox availability of the active compounds, likely due to improved solubilization and stabilization within the hydrated polymer matrix. Comparable results were obtained by Ghica et al. [60], who

reported DPPH, ABTS, and FRAP IC_{50} values of 805, 92, and 722 µg/mL, respectively, for ethanolic *Liquiritiae extractum*. The present hydrogels reached equivalent antioxidant capacity at an extract concentration of only 1 mg/mL, demonstrating efficient activity preservation within the semisolid medium. In another study, Sangkaew et al. [44] formulated a Thai herbal gel containing Gg and *Derris reticulata*, which showed a much weaker antioxidant profile (DPPH IC_{50} = 4.385 mg/mL) due to its mixed composition, lower extract potency, and higher test concentrations. Esmaeili et al. [61] recently characterized Iranian cultivated Gg genotypes rich in glycyrrhizic acid and glabridin, emphasizing that these flavonoids and triterpenoids are the key contributors to the plant's antioxidant and dermal-protective properties.

The differences among the assays (ABTS > DPPH > FRAP) reflect their distinct mechanisms and solvent environments. ABTS, being water-soluble and reactive toward both hydrophilic and lipophilic antioxidants, is particularly sensitive to the polyphenolic and flavonoid compounds in Gg. The aqueous nature of the hydrogels facilitates the interaction of these compounds with the ABTS radical, explaining the highest TE values obtained. In contrast, DPPH reacts more efficiently in organic media, which may limit radical accessibility in water-rich systems, while FRAP, based purely on electron transfer under acidic conditions, selectively detects strong reducing agents. Thus, the observed pattern confirms that the Gg hydrogels exhibit a broad antioxidant profile, combining both radical-scavenging and ferric-reducing mechanisms relevant to dermal protection against oxidative stress.

These results confirm that the Gg hydrogels preserved a strong, multi-mechanistic antioxidant profile after formulation. Such activity is particularly relevant for rosacea, where excessive ROS contribute to inflammation and vascular dysfunction. By efficiently neutralizing free radicals and reducing oxidative stress, these formulations may support the restoration of skin homeostasis and help mitigate rosacea-related inflammatory damage.

4.3. Antimicrobial Effects

The present results are in line with several reports highlighting the dual antioxidant and antimicrobial potential of Gg. Hamad et al. [62] showed that licorice root extract, incorporated into a functional yogurt, significantly enhanced both antioxidant capacity and resistance against foodborne pathogens, emphasizing the stability and bioactivity of its phenolic fraction in complex matrices. Comprehensive phytochemical reviews further support the key role of flavonoids such as glabridin, liquiritigenin, and licochalcone A, and triterpenes like glycyrrhizin, in mediating antioxidant, anti-inflammatory, and dermoprotective effects [18,47,63,64].

Rosacea is increasingly recognized as a disorder in which oxidative stress, neurovascular dysregulation, and alterations of the cutaneous microbiome interact to drive chronic inflammation [65,66]. Besides *Demodex*-associated changes, several bacterial species—including *Staphylococcus aureus*, *Streptococcus pyogenes*, and *Cutibacterium acnes*—have been involved in exacerbations of rosacea and other facial dermatoses [65,66].

In this context, the observed susceptibility of *S. pyogenes* and *C. acnes* to the Gg hydrogels (MIC 6.25–12.5 mg/mL) is clinically relevant. It should be noted that the reported MIC values refer to the hydrogel formulations containing 2% extract, rather than to the isolated Gg extract. Our data are consistent with previous reports showing that licorice root extracts and their major constituents exert antibacterial effects against Gram-positive skin pathogens. Comparable antimicrobial effects have been reported for licorice extract-based topical systems, with MIC values generally in the mg/mL range against Gram-positive skin-associated bacteria. These effects are typically moderate, and in the context of rosacea, are regarded as adjunctive to the antioxidant and anti-inflammatory properties of licorice extracts [47,60]. Several reviews and experimental studies attribute this activity mainly to

glabridin, licochalcone A, other prenylated flavonoids, and chalcones, which can disrupt bacterial membranes, interfere with energy metabolism, and modulate oxidative stress responses [18,62–64,67]. For instance, Singh et al. demonstrated that glabridin can affect oxidative stress pathways in multidrug-resistant *S. aureus* [67], while van Dinteren et al. [68] reported significant antimicrobial activity of prenylated flavonoids from liquorice roots against *Staphylococcus species*. Iqbal [47] also confirmed the notable antibacterial activity of Gg root extracts, supporting licorice as a source of bioactive antimicrobials. Although not classified as an infectious disease, the cutaneous microbiota can significantly influence rosacea severity by activating TLR-dependent pathways, amplifying inflammatory cytokines, and contributing to barrier dysfunction (Table 4) [65,66]. Several opportunistic or commensal bacteria—including *Staphylococcus aureus*, *Streptococcus pyogenes*, and *Cutibacterium acnes*—have been shown to modulate inflammation and neurovascular responses relevant to rosacea pathophysiology [69–71].

Table 4. Mechanistic implications of the tested bacterial strains in rosacea.

Bacteria	TLR Activated	Inflammation	Demonstrated Role in Rosacea	Observations
Streptococcus pyogenes	TLR2, TLR4	systemic	low/moderate	considered aggravating factor
Staphylococcus aureus	TLR2	local, strong	significant	contributing to pustule formation
Cutibacterium acnes	TLR2	local	secondary/indirect	observed especially in papule and pustule form

The moderate activity observed against *S. aureus* (MIC 50 mg/mL for both strains) is in line with these findings and with the generally higher intrinsic resistance of *S. aureus* compared with *C. acnes* or *S. pyogenes*, described for this species in earlier research [67,68]. Nevertheless, even partial growth inhibition can be valuable in a topical context, especially when combined with strong antioxidant and anti-inflammatory effects.

Finally, although none of these microbial strains are considered a direct etiological factor in rosacea, they may influence disease manifestations and severity through their effects on skin microbiome dysbiosis and the innate immune system. In this context, the antimicrobial activity of Gg—not necessarily bactericidal but also modulatory—may be beneficial in certain rosacea subtypes, particularly inflammatory and papulopustular forms.

4.4. Biocompatibility In Vitro on Keratinocytes

The biocompatibility of Gg-based hydrogel formulations was investigated through consecrated cytotoxicity assays: namely, a MTT assay for cell metabolic activity, the neutral red (NR) assay for lysosomal integrity, and the LDH assay for membrane disruption and necrosis. Together, these tests provide a comprehensive view of the cellular response to the tested formulations.

MTT assay results demonstrated concentration-dependent effects on keratinocyte viability, with the S1 formulation showing reduced cell viability below the 80% threshold at a concentration of 200 µg/mL. In contrast, the S2 formulation maintained cell viability above 84% when the same concentration of 200 µg/mL was used, indicating better cytocompatibility. Nevertheless, the slight decrease in HaCaT cell population may represent a key factor for acne treatment, providing the optimal conditions for its pathogenesis management. This pathogenesis is characterized by over-proliferation of keratinocytes under androgen stimulation and by aberrant keratinocyte proliferation responsible for the appearance of

comedones [72]. Thus, by using concentrations of 200 μg/mL of both samples, S1 and S2, the proper physiological skin conditions may be facilitated. On the other hand, rosacea is characterized by abnormal inflammatory responses to otherwise normal environmental stimuli. Recent evidence shows a clear connection between the physical skin barrier and the immune function response [69]. Keratinocytes are not merely structural components of the skin barrier; they also play a dynamic role in immune surveillance and the modulation of cutaneous inflammation. Upon exposure to environmental stressors such as ultraviolet (UV) radiation, pathogens, or mechanical injury, keratinocytes can act as immunologically active cells by producing a wide array of cytokines, chemokines, antimicrobial peptides, and danger signals [73]. Out of these, TLR and KLK5 are presently known to have a direct link to rosacea [74,75]. One of the most representative studies in this direction is conducted by Yamasaki et al. who showed the great impact that TLR2 mediators have in rosacea-affected skin, and how they are significantly increased in this case [69]. That is why a topical formulation for rosacea should aim to modulate keratinocyte activity in a controlled manner, rather than reduce their number, as this may help normalize multiple dysregulated pathways—including TLR2 signaling, KLK5 activity, and inflammatory mediator release.

These findings highlight the importance of modulating—rather than inhibiting—keratinocyte activity in the context of rosacea management. Keratinocytes play a central role in disease pathophysiology, and their targeted regulation may provide multiple therapeutic benefits. First, reducing keratinocyte hyperactivity can decrease the production of proinflammatory cytokines, thereby alleviating erythema and papulopustular lesions [73]. Second, limiting their activation helps suppress LL-37 peptide expression, a known contributor to inflammation, vasodilation, and aberrant angiogenesis in rosacea [73]. Third, controlling keratinocyte proliferation and differentiation supports epidermal homeostasis, improving barrier integrity, reducing trans-epidermal water loss, and enhancing resistance to external irritants [73]. Lastly, excessive keratinocyte turnover contributes to the accumulation of cellular debris, which favors Demodex proliferation; thus, modulating their expression may indirectly help normalize the skin microbiome [71].

Considering the current understanding of rosacea pathogenic mechanisms alongside the results of this MTT assay, it seems that Gg extract-loaded hydrogels modulate keratinocyte activity and proliferation, with many possible benefits for rosacea patients. Importantly, both S1_blank and S2_blank gels' cell viability is above 86.5% at the highest tested concentration, suggesting that the gel matrix itself exhibits minimal cytotoxicity and that the observed effects are mainly due to the extract.

These findings were further substantiated by the NR assay, which assesses damage to lysosomal membranes—an early indicator of cytotoxic stress. At lower concentrations (25–50 μg/mL), both formulations showed minimal lysosomal disruption. However, at a higher concentration of 200 μg/mL, a more pronounced cytotoxic response was observed. Both samples of S1 and S2 formulations induced similar lysosomal impairment—21.01% for S1 and 21.35% for S2.

LDH leakage, which is indicative of late-stage necrosis or membrane rupture, followed a similar pattern, indicating the same concentration-dependent effect. Notably, S1 induced LDH release of 24.7% at a concentration of 200 μg/mL, whereas S2 remained less cytotoxic (15.8%) under the same parameters (a concentration of 200 μg/mL and exposure time of 72 h).

These findings suggest that S2 gel formulation is comparatively less cytotoxic and more biocompatible with HaCaT keratinocytes, likely due to the difference in gel composition (namely the penetration enhancer) that may reduce cellular stress. These results align with previous studies that reported the relative safety of Gg components such as glycyrrhizin

and glabridin, which exert anti-inflammatory and cytoprotective effects when properly formulated [76,77].

Notably, the cytotoxic responses were not only formulation-dependent but also assay-specific, emphasizing the need for multiparametric evaluation in topical product development. The blank gel data further confirm that the observed effects originate from the active extract rather than the excipients, supporting the hydrogels' suitability as delivery systems with modifiable biological impact based on composition. Furthermore, both Gg-based gels (S1 and S2) emerge as promising candidates for rosacea management, given the disease's multifactorial pathogenesis involving vasoactive and neurocutaneous mechanisms [78].

4.5. Lack of Irritability and Angiogenic Activity in the CAM Assay

The absence of hemorrhage, lysis, or coagulation in the HET-CAM assay confirms the non-irritant nature of newly formulated hydrogels containing 2% methanolic Gg extract, in line with previous reports on licorice-derived formulations. Additionally, formulations containing glycyrrhizin or glycyrrhetinic acid have been shown to be well tolerated on topical application [79]. These results support the biocompatibility of Gg hydrogels and reinforce their potential for safe dermal application, particularly in conditions like rosacea where skin sensitivity and microvascular instability are key concerns.

Angiogenesis plays a central role in the pathophysiology of rosacea, particularly in the erythematotelangiectatic subtype, where persistent vasodilation and visible telangiectasia are hallmark features. Aberrant neovascularization is driven by inflammatory stimuli, such as increased levels of VEGF (vascular endothelial growth factor), LL-37 peptide, and ROS. This dysregulated angiogenic response not only sustains erythema and flushing, but also exacerbates inflammatory cell infiltration and skin sensitivity [80,81]. Therefore, therapeutic strategies that modulate angiogenic signaling—without compromising vascular integrity—are increasingly recognized as important in rosacea management.

Most common symptoms in rosacea patients are erythema and flushing of the facial skin, which can be attributed to various physiological changes, including increased skin blood flow, vasodilation, angiogenesis, elevated permeability, and upregulated levels of VEGF—a critical mediator of angiogenesis and vasopermeability [66]. Studies show that all rosacea types exhibit increased vascular endothelium factors. VEGF-A and VEGF-B regulate blood vessel formation, while VEGF-C and VEGF-D control lymphangiogenesis [82,83]. Vascular dysregulation involves several pro-angiogenic mediators, notably LL-37, which activates VEGF receptors and downstream pathways in epithelial cells, promoting angiogenesis and vascular proliferation [80].

In our study, both Gg-based hydrogel formulations led to a noticeable reduction in neovascularization on the CAM assay, as evidenced by the decreased capillary density and thinner vessels 48 h post-treatment. These findings support the anti-angiogenic potential of Gg root extract, consistent with prior reports. For instance, glycyrrhizin has been shown to modulate VEGF signaling and inhibit angiogenesis in hepatic and cutaneous models. For example, Pun et al. [84] demonstrated that glycyrrhizin had the ability to supress angiogenesis by VEGF signaling pathway regulation, in cirrhotic rats. This is particularly useful, since glycyrrhizin is known to be one of the major constituents in the Gg extract, and because VEGF has been shown to be upregulated in patients with rosacea. Furthermore, Jhanji et al. [85] studied the role of isoliquiritigenin in the process of ocular angiogenesis. Their experiment run ex ovo, on chick chorioallantoic membrane, showed that isoliquiritigenin suppressed VEGF-induced vessel growth in a dose-dependent way [85].

There are several other studies addressing the anti-angiogenic effect of either Gg extract or different molecules found in the *Glycyrrhiza* species. Sheela et al. confirmed

the angio-inhibitory activity of Gg by its inhibition of angiogenesis in in vivo assays, like peritoneal and chorioallantoic membrane assays [86]. In another study, Mohamed et al. showed that mice treated with Gg extract showed a decrease in the VEGF levels and microvessel density count [87]. Additionally, Gg extract has also been shown to reduce inflammatory and NO-producing cells [87]. These collective results reinforce the relevance of Gg in rosacea, where controlling aberrant angiogenesis is key to symptom management.

Taken together, the HET-CAM and CAM data indicate that the Gg hydrogels are both safe and capable of modulating angiogenic responses, supporting their relevance for managing the vascular and inflammatory components of rosacea. Although both formulations demonstrated anti-angiogenic activity without inducing irritation, the S2 formulation exhibited a more pronounced and sustained modulation of vascular development, suggesting a formulation-dependent enhancement of biological efficacy. This vascular modulation further suggests potential interactions with upstream innate immune pathways, forming the basis for subsequent investigation through immunohistochemical analysis.

4.6. Immunocytochemical Evaluation of Molecular Targets

The exacerbated immune response is one of the factors responsible for developing rosacea. The Toll-like receptor family is responsible for detecting external stimuli, such as microbes, UV rays, and injuries [88]. The overactivation of Toll-like receptor-2 (TLR2) throughout the keratinocytes has been shown to be one of the mechanisms of actions in rosacea [69,88]. Following the increase in TLR2, a cascade of processes caused by the release of pro-inflammatory cytokines and pro-angiogenic factors is triggered [89]. Furthermore, the activation of TLR-2 leads to the transcription of NF-κB, further increasing the transcription of cathelicidin-37 (LL37) and of kallikrein-5 [90]. All these factors have been studied and demonstrated to have a role in the mechanism of rosacea, being associated with symptoms like erythema, telangiectasia, and inflammation.

The IHC results provide morphological and molecular support regarding the cytocompatibility and safety profile of the formulations. The assessment of CD44, a cell surface glycoprotein involved in cell–cell interactions and adhesion, revealed that the S2 formulation preserves keratinocyte integrity better than S1 at high concentrations. The loss of CD44 intensity in S1 samples at 200 μg/mL correlates with the reduced cell viability observed in the MTT assay, suggesting that the propylene glycol-based formulation may disrupt membrane stability more aggressively than the Labrasol-based S2 formulation. Regarding vascular modulation, the low expression of VEGF in the treated keratinocytes aligns with the findings from the in ovo CAM assay. Since keratinocytes are a primary source of VEGF in inflammatory skin diseases, the lack of VEGF upregulation in the presence of the hydrogels suggests that the extract does not trigger angiogenic pathways in these cells.

It is necessary to highlight the specific technical constraints of this histological assessment. The analysis was conducted qualitatively to identify morphological and molecular safety patterns rather than quantitative efficacy. Additionally, the technical loss of the blank control cell blocks during processing precluded a direct side-by-side comparison between treated and vehicle-control samples. Consequently, the interpretation relies on the clear dose-dependent trends observed within the treated groups. Despite these limitations, the sequential preservation of CD44 and the specific, delayed onset of Caspase-3 expression only at higher concentrations provide valid internal evidence of the formulation's concentration-dependent biocompatibility.

Furthermore, the specific detection of Caspase-3 only at concentrations $\geq$ 100 μg/mL clarifies the mechanism of cell death. The presence of Caspase-3, combined with the cytoplasmic eosinophilia seen in HE staining, indicates that the extract induces apoptosis rather than uncontrolled necrosis at these concentrations. The ability of the S2 formulation

to maintain stronger CD44 expression and higher viability at 200 µg/mL compared to S1 confirms that the Labrasol-based hydrogel possesses a superior biocompatibility profile.

The biological effects observed in the present study can be rationalized by the well-documented molecular actions of the major constituents previously identified and quantitatively characterized in the methanolic Gg extract [21] incorporated into the hydrogel formulations evaluated here. Rosacea-related pathways involve oxidative stress, NF-κB/MAPK-mediated inflammation, and dysregulated angiogenesis [91]. Glycyrrhizin suppresses inflammatory signaling via inhibition of the HMGB1–TLR4/NF-κB axis and reduction in pro-inflammatory cytokines, while licorice flavonoids such as liquiritin and liquiritigenin modulate MAPK- and NF-κB-dependent pathways and oxidative stress. Notably, liquiritigenin exhibits anti-angiogenic activity through downregulation of HIF-1α and VEGF signaling, and liquiritin has been shown to significantly reduce VEGF expression and pathological microvessel formation through inhibition of p38 and JNK MAPK signaling [92]. Apigenin- and luteolin-based glycosides further contribute antioxidant and anti-inflammatory effects through ERK/NF-κB and iNOS modulation [93], supporting the biological relevance of licorice flavonoids for modulating inflammatory and vascular responses in rosacea-prone skin [94].

Collectively, the empirical data derived from this study indicate that hydrogels formulated with a chemically standardized Gg extract manifest a synergistic bioactive profile. By targeting key biological processes associated with inflammatory and vascular skin alterations—such as oxidative stress, inflammatory signaling, microbial imbalance, and vascular responses—the formulations show consistent and reproducible biological effects relevant to topical skincare applications. Importantly, the use of standardized extract composition and multiple assays strengthen the reliability of these findings, supporting the potential of licorice extract-loaded hydrogels as multifunctional topical candidates designed to address pathways commonly implicated in rosacea-prone and sensitive skin.

Despite the encouraging results, several limitations of the present study should be acknowledged. The biological evaluations were performed using general preclinical models that target key pathways relevant to rosacea, such as oxidative stress, inflammation, microbial imbalance, cytocompatibility, and angiogenesis. Therefore, the findings should be interpreted as preclinical support for topical formulations designed to modulate pathways implicated in rosacea. Future investigations should focus on more targeted experimental approaches, including advanced in vitro or ex vivo skin models and, ultimately, controlled clinical studies, to better define the relevance of Gg extract-loaded hydrogels and to define their precise role within a multimodal strategy for rosacea-prone skincare.

5. Conclusions

In this study, hydrogels containing a 2% methanolic extract of *Glycyrrhiza glabra* L. were successfully formulated and demonstrated rheological suitability, controlled release, and sustained epidermal permeation, consistent with high-quality topical delivery systems. The antioxidant, antimicrobial, and angiogenesis-modulating activities of the formulations highlight a multifunctional profile.

The hydrogels exhibited strong antioxidant capacity, moderate antibacterial activity against species that may contribute to rosacea flares, and an absence of irritation in HET-CAM testing. Additionally, reductions in neovascularization in the CAM assay and good biocompatibility in HaCaT cells further support their dermal safety and relevance for sensitive or reactive skin. Notably, comparative evaluation revealed formulation-dependent differences, with the Labrasol-based hydrogel (S2) consistently demonstrating superior cytocompatibility and a more pronounced and sustained modulation of angiogenic responses compared with the propylene glycol-based formulation (S1). The IHC analysis provides

crucial mechanistic insight, revealing that the hydrogels—particularly S2—maintain keratinocyte integrity through preserved CD44 expression and induce a controlled apoptotic turnover (mediated by Caspase-3) rather than necrosis at higher concentrations. Furthermore, the absence of VEGF upregulation at the cellular level aligns with the anti-angiogenic effects observed in ovo, supporting a profile that avoids exacerbating vascular triggers.

Overall, the present results position the Gg hydrogels as promising topical candidates capable of addressing several biological features associated with rosacea, including oxidative imbalance, inflammatory amplification, vascular reactivity, and microbiome-derived stimuli, while underscoring the critical role of formulation design.

Author Contributions: Conceptualization, I.S., Ș.A., and C.D.; methodology, Z.D., D.I.M., S.B., D.M., G.E.O., and I.S.; validation, Ș.A., C.A.D., and C.D.; investigation, I.S., Z.D., A.C., C.G.W., D.M., Z.D., and G.E.O.; data curation, I.S., Z.D., L.B., A.C., C.G.W., A.O.D., S.B., D.M., and G.E.O.; writing—original draft preparation, I.S., L.B., and A.O.D.; writing—review and editing, I.S., L.B., Ș.A., and C.D.; visualization, L.B. and D.I.M.; and supervision, Ș.A. and C.D. All authors have read and agreed to the published version of the manuscript.

Funding: We would like to acknowledge "Victor Babeș" University of Medicine and Pharmacy Timi;oara, Romania, for their support in covering the costs of publication for this research paper.

Institutional Review Board Statement: Not applicable.

Informed Consent Statement: Not applicable.

Data Availability Statement: The original contributions presented in this study are included in the article. Further inquiries can be directed to the corresponding author.

Acknowledgments: Doctoral School of Pharmacy, "Victor Babeș" University of Medicine and Pharmacy Timișoara.

Conflicts of Interest: The authors declare no conflicts of interest.

References

1. Saric, S.; Clark, A.K.; Sivamani, R.K.; Lio, P.A.; Lev-Tov, H.A. The Role of Polyphenols in Rosacea Treatment: A Systematic Review. *J. Altern. Complement. Med.* **2017**, *23*, 920–929. [CrossRef]
2. Aroni, K.; Tsagroni, E.; Kavantzas, N.; Patsouris, E.; Ioannidis, E. A Study of the Pathogenesis of Rosacea: How Angiogenesis and Mast Cells May Participate in a Complex Multifactorial Process. *Arch. Dermatol. Res.* **2008**, *300*, 125–131. [CrossRef]
3. van Zuuren, E.J.; Arents, B.W.M.; van der Linden, M.M.D.; Vermeulen, S.; Fedorowicz, Z.; Tan, J. Rosacea: New Concepts in Classification and Treatment. *Am. J. Clin. Dermatol.* **2021**, *22*, 457–465. [CrossRef]
4. Dall'Oglio, F.; Nasca, M.R.; Micali, G. Emerging Topical Drugs for the Treatment of Rosacea. *Expert. Opin. Emerg. Drugs* **2021**, *26*, 27–38. [CrossRef]
5. Geng, R.S.Q.; Sood, S.; Hua, N.; Chen, J.; Sibbald, R.G.; Sibbald, C. Efficacy of Treatments in Reducing Inflammatory Lesion Count in Rosacea: A Systematic Review. *J. Cutan. Med. Surg.* **2024**, *28*, 352. [CrossRef] [PubMed]
6. Geng, R.S.Q.; Bourkas, A.N.; Mufti, A.; Sibbald, R.G. Rosacea: Pathogenesis and Therapeutic Correlates. *J. Cutan. Med. Surg.* **2024**, *28*, 178. [CrossRef] [PubMed]
7. Li, Y.; Xie, H.; Deng, Z.; Wang, B.; Tang, Y.; Zhao, Z.; Yuan, X.; Zuo, Z.; Xu, S.; Zhang, Y.; et al. Tranexamic Acid Ameliorates Rosacea Symptoms Through Regulating Immune Response and Angiogenesis. *Int. Immunopharmacol.* **2019**, *67*, 326–334. [CrossRef] [PubMed]
8. Buhl, T.; Sulk, M.; Nowak, P.; Buddenkotte, J.; McDonald, I.; Aubert, J.; Carlavan, I.; Déret, S.; Reiniche, P.; Rivier, M.; et al. Molecular and Morphological Characterization of Inflammatory Infiltrate in Rosacea Reveals Activation of Th1/Th17 Pathways. *J. Investig. Dermatol.* **2015**, *135*, 2198–2208. [CrossRef]
9. Makarska-Białokoz, M. History and significance of phytotherapy in the human history. The development of phytotherapy from the Middle Ages to modern times. *Arch. Physiother. Glob. Res.* **2020**, *24*, 17–22. [CrossRef]
10. Leite, P.M.; Camargos, L.M.; Castilho, R.O. Recent Progess in Phytotherapy: A Brazilian Perspective. *Eur. J. Integr. Med.* **2021**, *41*, 101270. [CrossRef]

11. Paiva-Santos, A.C.; Gonçalves, T.; Peixoto, D.; Pires, P.C.; Velsankar, K.; Jha, N.K.; Chavda, V.P.; Mohammad, I.S.; Cefali, L.C.; Mazzola, P.G.; et al. Rosacea Topical Treatment and Care: From Traditional to New Drug Delivery Systems. *Mol. Pharm.* **2023**, *20*, 3804–3828. [CrossRef]
12. Colalto, C.; Leite, P.M.; Camargos, L.M.; Castilho, R.O.; Lopes, C.M.C.; Lazzarini, J.R.; Soares, J.M.; Baracat, E.C.; Miraldi, E.; Baini, G.; et al. Recent Progess in Phytotherapy: A Brazilian Perspective. *J. Siena Acad. Sci.* **2018**, *10*, 7–12. [CrossRef]
13. Wahab, S.; Annadurai, S.; Abullais, S.S.; Das, G.; Ahmad, W.; Ahmad, M.F.; Kandasamy, G.; Vasudevan, R.; Ali, M.S.; Amir, M. *Glycyrrhiza glabra* (Licorice): A Comprehensive Review on Its Phytochemistry, Biological Activities, Clinical Evidence and Toxicology. *Plants* **2021**, *10*, 2751. [CrossRef] [PubMed]
14. Alobaidi, A.H.; Hamad, E.S.; Alsamarai, A.M.; Kudair, K.A. Evaluation of *Glycyrrhiza glabra* Cream as Treatmentfor Melasma. *Evid.-Based Strateg. Herbal. Med. Psychiatr. Disord. Emerg. Med.* **2015**. [CrossRef]
15. Celano, R.; Docimo, T.; Piccinelli, A.L.; Rizzo, S.; Campone, L.; Di Sanzo, R.; Carabetta, S.; Rastrelli, L.; Russo, M. Specialized Metabolite Profiling of Different *Glycyrrhiza glabra* Organs by Untargeted UHPLC-HRMS. *Ind. Crops Prod.* **2021**, *170*, 113688. [CrossRef]
16. Kaur, R.; Kaur, H.; Dhindsa, A.S. *Glycyrrhiza glabra*: A Phytopharmacological Review. *Int. J. Pharm. Sci. Res.* **2013**, *4*, 2470. [CrossRef]
17. Sharma, D.; Namdeo, P.; Singh, P. Phytochemistry and Pharmacological Studies of *Glycyrrhiza glabra*: A Medicinal Plant Review. *Int. J. Pharm. Sci. Rev. Res.* **2021**, *67*, 187–194. [CrossRef]
18. Sharma, V.; Katiyar, A.; Agrawal, R.C. Glycyrrhiza glabra: Chemistry and Pharmacological Activity. In *Sweeteners*; Springer: Cham, The Netherland, 2017; Volume 87. [CrossRef]
19. Babich, O.; Ivanova, S.; Ulrikh, E.; Popov, A.; Larina, V.; Frolov, A.; Prosekov, A. Study of the Chemical Composition and Biologically Active Properties of *Glycyrrhiza glabra* Extracts. *Life* **2022**, *12*, 1772. [CrossRef]
20. Thakur, D.; Jain, A.; Ghoshal, G. Evaluation of Phytochemical, Antioxidant and Antimicrobial Properties of Glycyrrhizin Extracted from Roots of *Glycyrrhiza glabra*. *J. Sci. Ind. Res.* **2016**, *75*, 487–494.
21. Semenescu, I.; Avram, S.; Similie, D.; Minda, D.; Diaconeasa, Z.; Muntean, D.; Lazar, A.E.; Gurgus, D.; Danciu, C. Phytochemical, Antioxidant, Antimicrobial and Safety Profile of *Glycyrrhiza glabra* L. Extract Obtained from Romania. *Plants* **2024**, *13*, 3265. [CrossRef]
22. Fisk, W.A.; Lev-Tov, H.A.; Clark, A.K.; Sivamani, R.K. Phytochemical and Botanical Therapies for Rosacea: A Systematic Review. *Phytother. Res.* **2015**, *29*, 1439–1451. [CrossRef]
23. Rigopoulos, D.; Kalogeromitros, D.; Gregoriou, S.; Pacouret, J.M.; Koch, C.; Fisher, N.; Bachmann, K.; Brown, M.; Schwarz, E.; Camel, E.; et al. Randomized Placebo-Controlled Trial of a Flavonoid-Rich Plant Extract-Based Cream in the Treatment of Rosacea. *J. Eur. Acad. Dermatol. Venereol.* **2005**, *19*, 564–568. [CrossRef] [PubMed]
24. Bisht, D.; Rashid, M.; Arya, R.K.K.; Kumar, D.; Chaudhary, S.K.; Rana, V.S.; Sethiya, N.K. Revisiting Liquorice (*Glycyrrhiza glabra* L.) as Anti-Inflammatory, Antivirals and Immunomodulators: Potential Pharmacological Applications with Mechanistic Insight. *Phytomedicine Plus* **2022**, *2*, 100206. [CrossRef]
25. Quality and Equivalence of Locally Applied, Locally Acting Cutaneous Products-Scientific Guideline | European Medicines Agency (EMA). Available online: https://www.ema.europa.eu/en/quality-equivalence-locally-applied-locally-acting-cutaneous-products-scientific-guideline (accessed on 17 December 2025).
26. Kligman, A.M.; Christophers, E. Preparation of isolated sheets of human stratum corneum. *Arch. Dermatol.* **1963**, *88*, 702–705. [CrossRef]
27. Brand-Williams, W.; Cuvelier, M.E.; Berset, C. Use of a Free Radical Method to Evaluate Antioxidant Activity. *LWT-Food Sci. Technol.* **1995**, *28*, 25–30. [CrossRef]
28. Benzie, I.F.F.; Strain, J.J. The Ferric Reducing Ability of Plasma (FRAP) as a Measure of "Antioxidant Power": The FRAP Assay. *Anal. Biochem.* **1996**, *239*, 70–76. [CrossRef] [PubMed]
29. Ozgen, M.; Reese, R.N.; Tulio, A.Z.; Scheerens, J.C.; Miller, A.R. Modified 2,2-Azino-Bis-3-Ethylbenzothiazoline-6-Sulfonic Acid (Abts) Method to Measure Antioxidant Capacity of Selected Small Fruits and Comparison to Ferric Reducing Antioxidant Power (FRAP) and 2,2′-Diphenyl-1-Picrylhydrazyl (DPPH) Methods. *J. Agric. Food Chem.* **2006**, *54*, 1151–1157. [CrossRef]
30. European Committee on Antimicrobial Susceptibility Testing (EUCAST). Media Preparation for EUCAST Disk Diffusion Testing and for Determination of MIC Values by the Broth Microdilution Method. 2022. Available online: http://www.eucast.org (accessed on 9 September 2025).
31. Patel, J.B. *Performance Standards for Antimicrobial Susceptibility Testing*; Clinical and Laboratory Standards Institute: Wayne, PA, USA, 2016.
32. Moacă, E.A.; Watz, C.G.; Socoliuc, V.; Racoviceanu, R.; Păcurariu, C.; Ianoş, R.; Cîntă-Pînzaru, S.; Tudoran, L.B.; Nekvapil, F.; Iurciuc, S.; et al. Biocompatible Magnetic Colloidal Suspension Used as a Tool for Localized Hyperthermia in Human Breast Adenocarcinoma Cells: Physicochemical Analysis and Complex In Vitro Biological Profile. *Nanomaterials* **2021**, *11*, 1189. [CrossRef]

33. Ghițu, A.; Schwiebs, A.; Radeke, H.H.; Avram, S.; Zupko, I.; Bor, A.; Pavel, I.Z.; Dehelean, C.A.; Oprean, C.; Bojin, F.; et al. A Comprehensive Assessment of Apigenin as an Antiproliferative, Proapoptotic, Antiangiogenic and Immunomodulatory Phytocompound. *Nutrients* **2019**, *11*, 858. [CrossRef]
34. Corina, D.; Delia, M.; Ersilia, A.; Claudia, F.; Camelia, O.; Istvan, Z.; Andrea, B.; Daliana, M.; Maria, P.; Valentina, B.; et al. Phytochemical Characterization and Evaluation of the Antimicrobial, Antiproliferative and Pro-Apoptotic Potential of Ephedra Alata Decne. Hydroalcoholic Extract against the MCF-7 Breast Cancer Cell Line. *Molecules* **2018**, *24*, 13. [CrossRef]
35. Avram, Ș.; Bora, L.; Vlaia, L.L.; Muț, A.M.; Olteanu, G.E.; Olariu, I.; Magyari-Pavel, I.Z.; Minda, D.; Diaconeasa, Z.; Sfirloaga, P.; et al. Cutaneous Polymeric-Micelles-Based Hydrogel Containing *Origanum vulgare* L. Essential Oil: In Vitro Release and Permeation, Angiogenesis, and Safety Profile In Ovo. *Pharmaceuticals* **2023**, *16*, 940. [CrossRef]
36. ICCVAM Test Method Validation Report: Current Validation Status of In Vitro Test Methods Proposed for Identifying Eye Injury Hazard Potential of Chemicals and Products-Vol 1|EURL ECVAM-TSAR. Available online: https://tsar.jrc.ec.europa.eu/content/iccvam-test-method-validation-report-current-validation-status-vitro-test-methods-proposed-1 (accessed on 15 November 2025).
37. Luepke, N.P. Hen's Egg Chorioallantoic Membrane Test for Irritation Potential. *Food Chem. Toxicol.* **1985**, *23*, 287–291. [CrossRef]
38. Saurat, J.-H.; Halioua, B.; Baissac, C.; Cullell, N.P.; Ben Hayoun, Y.; Aroman, M.S.; Taieb, C.; Skayem, C. Epidemiology of Acne and Rosacea: A Worldwide Global Study. *J. Am. Acad. Dermatol.* **2024**, *90*, 1016–1018. [CrossRef] [PubMed]
39. Chang, H.C.; Huang, Y.C.; Lien, Y.J.; Chang, Y.S. Association of Rosacea with Depression and Anxiety: A Systematic Review and Meta-Analysis. *J. Affect. Disord.* **2022**, *299*, 239–245. [CrossRef] [PubMed]
40. Lonne-Rahm, S.; Nordlind, K.; Edström, D.W.; Ros, A.M.; Berg, M. Laser Treatment of Rosacea: A Pathoetiological Study. *Arch. Dermatol.* **2004**, *140*, 1345–1349. [CrossRef]
41. Fisher, G.W.; Travers, J.B.; Rohan, C.A. Rosacea Pathogenesis and Therapeutics: Current Treatments and a Look at Future Targets. *Front. Med.* **2023**, *10*, 1292722. [CrossRef] [PubMed]
42. Sieradocha, K.; Jedlikowska, W.; Furlepa, N. Role of Inflammatory Pathways in the Development of Rosacea. *J. Educ. Health Sport* **2024**, *71*, 56142. [CrossRef]
43. Zhang, Y.Q.; Liang, R.; Liu, C.; Yang, C. Improved Stability and Skin Penetration through Glycethosomes Loaded with Glycyrrhetinic Acid. *Int. J. Cosmet. Sci.* **2022**, *44*, 249–261. [CrossRef]
44. Sangkaew, W.; Sianglum, W.; Wunnoo, S.; Voravuthikunchai, S.P.; Joycharat, N. Bioactive Substance Contents and Therapeutic Potential for Skin Inflammation of an Herbal Gel Containing Derris Reticulata and *Glycyrrhiza glabra*. *Pharm. Biol.* **2024**, *62*, 648–658. [CrossRef]
45. Yang, R.; Yuan, B.C.; Ma, Y.S.; Zhou, S.; Liu, Y. The Anti-Inflammatory Activity of Licorice, a Widely Used Chinese Herb. *Pharm. Biol.* **2017**, *55*, 5–18. [CrossRef]
46. Tuli, H.S.; Garg, V.K.; Mehta, J.K.; Kaur, G.; Mohapatra, R.K.; Dhama, K.; Sak, K.; Kumar, A.; Varol, M.; Aggarwal, D.; et al. Licorice (*Glycyrrhiza glabra* L.)-Derived Phytochemicals Target Multiple Signaling Pathways to Confer Oncopreventive and Oncotherapeutic Effects. *Onco Targets Ther.* **2022**, *15*, 1419. [CrossRef]
47. Iqbal, Z. Antioxidant and Antibacterial Activity of Organic Extracts of Roots of *Glycyrrhiza glabra* Linn. *Plant* **2017**, *5*, 68. [CrossRef]
48. Bhusal, S.; Sharma, K.R. Evaluation of Antioxidant and Antibacterial Activity of *Glycyrrhiza glabra* Root Extracts. *Asian J. Pharm. Clin. Res.* **2020**, 166–170. [CrossRef]
49. Fatoki, T.H.; Ajiboye, B.O.; Aremu, A.O. In Silico Evaluation of the Antioxidant, Anti-Inflammatory, and Dermatocosmetic Activities of Phytoconstituents in Licorice (*Glycyrrhiza glabra* L.). *Cosmetics* **2023**, *10*, 69. [CrossRef]
50. Graebin, C.S. The Pharmacological Activities of Glycyrrhizinic Acid ("Glycyrrhizin") and Glycyrrhetinic Acid. In *Sweeteners*; Springer: Berlin/Heidelberg, Germany, 2018; Volume 245. [CrossRef]
51. Semenescu, I.; Avram, Ș.; Bora, L.; Berkó, S.; Minda, D.; Danciu, C. Antioxidant Activity of 2% *G. glabra* L. Hydrogels for Potential Use in Oxidative Stress-Related Skin Conditions. *Proceedings* **2025**, *127*, 24. [CrossRef]
52. Lai, W.F.; Rogach, A.L. Hydrogel-Based Materials for Delivery of Herbal Medicines. *ACS Appl. Mater. Interfaces* **2017**, *9*, 11309–11320. [CrossRef]
53. Nawaz, A.; Ullah, S.; Alnuwaiser, M.A.; Rehman, F.U.; Selim, S.; Al Jaouni, S.K.; Farid, A. Formulation and Evaluation of Chitosan-Gelatin Thermosensitive Hydrogels Containing 5FU-Alginate Nanoparticles for Skin Delivery. *Gels* **2022**, *8*, 537. [CrossRef] [PubMed]
54. Singhvi, G.; Hans, N.; Shiva, N.; Kumar Dubey, S. Xanthan Gum in Drug Delivery Applications. *Nat. Polysacch. Drug Deliv. Biomed. Appl.* **2019**, 121–144. [CrossRef]
55. Yaseen, M.R.; Faisal, G.G.; Fuaat, A.A.; Affandi, K.A.; Alallam, B.; Mohd Nasir, M.H. Preparation of Euyrycoma Longifolia Jack (E.L) Tongkat Ali (Ta) Root Extract Hydrogel for Wound Application. *Pharmacogn. J.* **2021**, *13*, 1456–1463. [CrossRef]
56. Mees, M.A.; Boone, F.; Bouwen, T.; Vanaerschot, F.; Titeca, C.; Vikkula, H.K.; Catrysse, L.; Vananroye, A.; Koos, E.; Alexandris, S.; et al. Glycyrrhizin-Based Hydrogels Accelerate Wound Healing of Normoglycemic and Diabetic Mouse Skin. *Pharmaceutics* **2023**, *15*, 27. [CrossRef]

57. Armanini, D.; Fiore, C.; Mattarello, M.J.; Bielenberg, J.; Palermo, M. History of the Endocrine Effects of Licorice. *Exp. Clin. Endocrinol. Diabetes* **2002**, *110*, 257–261. [CrossRef] [PubMed]
58. Carmona-Rivera, C.; Kaplan, M.J. Low Density Granulocytes: A Distinct Class of Neutrophils in Systemic Autoimmunity. *Semin. Immunopathol.* **2013**, *35*, 455. [CrossRef] [PubMed]
59. Nguyen, G.; Torres, A. Systemic Antioxidants and Skin Health. *J. Drugs Dermatol.* **2012**, *11*, e1-4. [PubMed]
60. Ghica, A.; Drumea, V.; Moroșan, A.; Mihaiescu, D.E.; Costea, L.; Luță, E.A.; Mihai, D.P.; Balaci, D.T.; Fița, A.C.; Olaru, O.T.; et al. Phytochemical Screening and Antioxidant Potential of Selected Extracts from Betula Alba Var. Pendula Roth., *Glycyrrhiza glabra* L., and *Avena sativa* L. *Plants* **2023**, *12*, 2510. [CrossRef]
61. Esmaeili, H.; Mirjalili, M.H.; Karami, A.; Nejad Ebrahimi, S. Introducing the Glycyrrhizic Acid and Glabridin Rich Genotypes from the Cultivated Iranian Licorice (*Glycyrrhiza glabra* L.) Populations to Exploit in Production Systems. *Sci. Rep.* **2024**, *14*, 11034. [CrossRef]
62. Hamad, G.M.; Elaziz, A.I.A.; Hassan, S.A.; Shalaby, M.A.; Mohdaly, A.A.A.A. Chemical Composition, Antioxidant, Antimicrobial and Anticancer Activities of Licorice (*Glycyrrhiza glabra* L.) Root and Its Application in Functional Yoghurt. *J. Food Nutr. Res.* **2020**, *8*, 707–715. [CrossRef]
63. Zhang, J.; Wu, X.; Zhong, B.; Liao, Q.; Wang, X.; Xie, Y.; He, X. Review on the Diverse Biological Effects of Glabridin. *Drug Des. Devel Ther.* **2023**, *17*, 15. [CrossRef]
64. Esmail Al-Snafi, A. *Glycyrrhiza glabra*: A Phytochemical and Pharmacological Review. *IOSR J. Pharm.* **2018**, *8*, 1–17.
65. Two, A.M.; Wu, W.; Gallo, R.L.; Hata, T.R. Rosacea: Part I. Introduction, Categorization, Histology, Pathogenesis, and Risk Factors. *J. Am. Acad. Dermatol.* **2015**, *72*, 749–758. [CrossRef] [PubMed]
66. Chen, C.; Wang, P.; Zhang, L.; Liu, X.; Zhang, H.; Cao, Y.; Wang, X.; Zeng, Q. Exploring the Pathogenesis and Mechanism-Targeted Treatments of Rosacea: Previous Understanding and Updates. *Biomedicines* **2023**, *11*, 2153. [CrossRef]
67. Singh, V.; Pal, A.; Darokar, M.P. A Polyphenolic Flavonoid Glabridin: Oxidative Stress Response in Multidrug-Resistant Staphylococcus Aureus. *Free Radic. Biol. Med.* **2015**, *87*, 48–57. [CrossRef]
68. van Dinteren, S.; Meijerink, J.; Witkamp, R.; van Ieperen, B.; Vincken, J.P.; Araya-Cloutier, C. Valorisation of Liquorice (*Glycyrrhiza*) Roots: Antimicrobial Activity and Cytotoxicity of Prenylated (Iso)Flavonoids and Chalcones from Liquorice Spent (*G. Glabra*, *G. Inflata*, and *G. Uralensis*). *Food Funct.* **2022**, *13*, 12105–12120. [CrossRef]
69. Yamasaki, K.; Kanada, K.; MacLeod, D.T.; Borkowski, A.W.; Morizane, S.; Nakatsuji, T.; Cogen, A.L.; Gallo, R.L. TLR2 Expression Is Increased in Rosacea and Stimulates Enhanced Serine Protease Production by Keratinocytes. *J. Investig. Dermatol.* **2011**, *131*, 688–697. [CrossRef]
70. Peng, L.; Jiang, J.; Chen, T.; Xu, D.; Hou, F.; Huang, Q.; Peng, Y.; Ye, C.; Hu, D.L.; Fang, R. Toxic Shock Syndrome Toxin 1 Induces Immune Response via the Activation of NLRP3 Inflammasome. *Toxins* **2021**, *13*, 68. [CrossRef]
71. Thompson, K.G.; Rainer, B.M.; Antonescu, C.; Florea, L.; Mongodin, E.F.; Kang, S.; Chien, A.L. Comparison of the Skin Microbiota in Acne and Rosacea. *Exp. Dermatol.* **2021**, *30*, 1375–1380. [CrossRef]
72. González-Mondragón, E.A.; Ganoza-Granados, L.D.C.; Toledo-Bahena, M.E.; Valencia-Herrera, A.M.; Duarte-Abdala, M.R.; Camargo-Sánchez, K.A.; Mena-Cedillos, C.A. Acne and Diet: A Review of Pathogenic Mechanisms. *Bol. Med. Hosp. Infant. Mex.* **2022**, *79*, 83–90. [CrossRef] [PubMed]
73. Two, A.M.; Del Rosso, J.Q. Kallikrein 5-Mediated Inflammation in Rosacea: Clinically Relevant Correlations with Acute and Chronic Manifestations in Rosacea and How Individual Treatments May Provide Therapeutic Benefit. *J. Clin. Aesthet. Dermatol.* **2014**, *7*, 20. [PubMed]
74. Roh, K.B.; Jang, Y.; Cho, E.; Park, D.; Kweon, D.H.; Jung, E. Chlorogenic Acid Isomers Isolated from Artemisia Lavandulaefolia Exhibit Anti-Rosacea Effects In Vitro. *Biomedicines* **2022**, *10*, 463. [CrossRef]
75. Matsubara, Y.; Matsumoto, T.; Koseki, J.; Kaneko, A.; Aiba, S.; Yamasaki, K. Inhibition of Human Kallikrein 5 Protease by Triterpenoids from Natural Sources. *Molecules* **2017**, *22*, 1829. [CrossRef] [PubMed]
76. Shah, S.L.; Wahid, F.; Khan, N.; Farooq, U.; Shah, A.J.; Tareen, S.; Ahmad, F.; Khan, T. Inhibitory Effects of *Glycyrrhiza glabra* and Its Major Constituent Glycyrrhizin on Inflammation-Associated Corneal Neovascularization. *Evid.-Based Complement. Altern. Med.* **2018**, *2018*, 8438101. [CrossRef]
77. Parlar, A.; Arslan, S.O.; Çam, S.A. Glabridin Alleviates Inflammation and Nociception in Rodents by Activating BKCa Channels and Reducing NO Levels. *Biol. Pharm. Bull.* **2020**, *43*, 884–897. [CrossRef]
78. Picardo, M.; Eichenfield, L.F.; Tan, J. Acne and Rosacea. *Dermatol. Ther.* **2017**, *7*, 43–52. [CrossRef] [PubMed]
79. Zhao, Z.-W.; Cai, M.-H.; Wang, P.; Wang, D.-D.; Liu, Y.; Chen, Y.-Z. Application of Glycyrrhizic Acid and Glycyrrhetinic Acid in the Drug Delivery System. *J. Drug Deliv. Sci. Technol.* **2024**, *97*, 105754. [CrossRef]
80. Yang, F.; Wang, L.; Song, D.; Zhang, L.; Wang, X.; Du, D.; Jiang, X. Signaling Pathways and Targeted Therapy for Rosacea. *Front. Immunol.* **2024**, *15*, 1367994. [CrossRef]
81. Lee, H.J.; Hong, Y.J.; Kim, M. Angiogenesis in Chronic Inflammatory Skin Disorders. *Int. J. Mol. Sci.* **2021**, *22*, 12035. [CrossRef]

82. Schwab, V.D.; Sulk, M.; Seeliger, S.; Nowak, P.; Aubert, J.; Mess, C.; Rivier, M.; Carlavan, I.; Rossio, P.; Metze, D.; et al. Neurovascular and Neuroimmune Aspects in the Pathophysiology of Rosacea. *J. Investig. Dermatol. Symp. Proc.* **2011**, *15*, 53–62. [CrossRef]
83. Huggenberger, R.; Detmar, M. The Cutaneous Vascular System in Chronic Skin Inflammation. *J. Investig. Dermatol. Symp. Proc.* **2011**, *15*, 24–32. [CrossRef]
84. Pun, C.K.; Huang, H.C.; Chang, C.C.; Chuang, C.L.; Yen, C.H.; Hsu, S.J.; Lee, F.Y.; Hou, M.C.; Huang, Y.H. Glycyrrhizin Attenuates Portal Hypertension and Collateral Shunting via Inhibition of Extrahepatic Angiogenesis in Cirrhotic Rats. *Int. J. Mol. Sci.* **2021**, *22*, 7662. [CrossRef]
85. Jhanji, V.; Liu, H.; Law, K.; Lee, V.Y.W.; Huang, S.F.; Pang, C.P.; Yam, G.H.F. Isoliquiritigenin from Licorice Root Suppressed Neovascularisation in Experimental Ocular Angiogenesis Models. *Br. J. Ophthalmol.* **2011**, *95*, 1309–1315. [CrossRef]
86. Sheela, M.L.; Ramakrishna, M.K.; Salimath, B.P. Angiogenic and Proliferative Effects of the Cytokine VEGF in Ehrlich Ascites Tumor Cells Is Inhibited by *Glycyrrhiza glabra*. *Int. Immunopharmacol.* **2006**, *6*, 494–498. [CrossRef] [PubMed]
87. Mohamed, D.D.; Mahrous, H.; Khalil, H.; Ibrahim, I.A.; Mohamed, D.D.; Keshk, O.S.; Nada, A.H.; El Maksoud, A.I.A. Regulation of Angiogenesis and Inflammatory Pathways by Glycyrrhizic Acid. *Egypt. J. Dermatol. Venereol.* **2024**, *44*, 80–89. [CrossRef]
88. Chen, L.-X.-Y.; Hao, P.-S. The Role of Skin Barrier and Immune Abnormalities in the Pathogenesis of Rosacea. *Clin. Exp. Med.* **2025**, *25*, 324. [CrossRef] [PubMed]
89. Yuan, X.; Li, J.; Li, Y.; Deng, Z.; Zhou, L.; Long, J.; Tang, Y.; Zuo, Z.; Zhang, Y.; Xie, H. Artemisinin, a Potential Option to Inhibit Inflammation and Angiogenesis in Rosacea. *Biomed. Pharmacother.* **2019**, *117*, 109181. [CrossRef]
90. Semenescu, I.; Similie, D.; Diaconeasa, Z.; Danciu, C. Recent Advances in the Management of Rosacea through Natural Compounds. *Pharmaceuticals* **2024**, *17*, 212. [CrossRef] [PubMed]
91. Andrusiewicz, A.; Khimuk, S.; Mijas, D.; Shmorhun, B.; Nowicka, D.; Andrusiewicz, A.; Khimuk, S.; Mijas, D.; Shmorhun, B.; Nowicka, D. Molecular Mechanisms in the Etiopathology of Rosacea—Systematic Review. *Int. J. Mol. Sci.* **2025**, *26*, 11292. [CrossRef]
92. Zhai, K.F.; Duan, H.; Cui, C.Y.; Cao, Y.Y.; Si, J.L.; Yang, H.J.; Wang, Y.C.; Cao, W.G.; Gao, G.Z.; Wei, Z.J. Liquiritin from Glycyrrhiza Uralensis Attenuating Rheumatoid Arthritis via Reducing Inflammation, Suppressing Angiogenesis, and Inhibiting MAPK Signaling Pathway. *J. Agric. Food Chem.* **2019**, *67*, 2856–2864. [CrossRef]
93. Wu, Y.; Wang, Z.; Du, Q.; Zhu, Z.; Chen, T.; Xue, Y.; Wang, Y.; Zeng, Q.; Shen, C.; Jiang, C.; et al. Pharmacological Effects and Underlying Mechanisms of Licorice-Derived Flavonoids. *Evid.-Based Complement. Altern. Med.* **2022**, *2022*, 9523071. [CrossRef]
94. Fatima, I.; Sahar, A.; Tariq, A.; Naz, T.; Usman, M. Exploring the Role of Licorice and Its Derivatives in Cell Signaling Pathway NF-KB and MAPK. *J. Nutr. Metab.* **2024**, *2024*, 9988167. [CrossRef]

Disclaimer/Publisher's Note: The statements, opinions and data contained in all publications are solely those of the individual author(s) and contributor(s) and not of MDPI and/or the editor(s). MDPI and/or the editor(s) disclaim responsibility for any injury to people or property resulting from any ideas, methods, instructions or products referred to in the content.